

Dear Editor Michiel van den Broeke,

Thank you for your letter on October 29 inviting revisions to our manuscript, ***“Supraglacial meltwater routing through internally drained catchments on the Greenland Ice Sheet surface.”***

We are pleased to state that we have complied with all of the requests made by the two reviewers. A stepwise, detailed response to all comments is as follows:

Reviewer #1

General comments:

Supraglacial catchment hydrology controls the seasonal and daily inputs of surface meltwater to subglacial catchments, thus modulating subglacial channel evolution and, by extension, ice sheet response to surface melt. However, very little is known about the routing of water within a supraglacial catchment, and a dearth of empirical data hampers efforts to generalize methods for constructing moulin hydrographs. This paper is a meaningful and logical use of a unique in-situ measured moulin hydrograph, which is combined with traditional hydrological theory to infer the distribution of water routing within different spatial process domains in a supraglacial Internally Drained Catchment (IDC). It is largely a methods paper, but also provides insight into the relative importance and roles of the different hydrological spatial domains in routing flow, as well as how this importance varies seasonally with the evolution of the supraglacial drainage network.

The contributions of this paper to the field are:

1. Unique empirical data on moulin hydrology
2. Methodological advancements on moulin discharge derivations that emphasize the importance of considering the different hydrological processes at work within spatially distinct process domains
3. Insights into the importance of the seasonal evolution of different parts of the supraglacial drainage networks on modifying moulin hydrographs

The contributions of this paper might be enhanced in the following ways:

1. (“Because this paper is largely a method paper and relies on empirical data that is available for few supraglacial catchments, it would benefit from a discussion of the choice to use the rescaled width function relative to other methods for deriving synthetic unit hydrographs. What are the practical considerations of this method, and why is it best suited for the supraglacial environment? ”)

Reply: The Surface Routing and Lake Filling (SRLF) model is the first to attempt routing of surface meltwater downslope (Arnold et al., 1998). More recently, the Snyder Synthetic Unit Hydrograph (SUH) was used to derive moulin hydrographs (Smith et al., 2017). Both methods simulate observed moulin hydrographs reasonably well, but they cannot insightfully reveal the physical process of surface meltwater routing. Recently, permeable weathering crust was found on the Greenland bare-ice surface (Cooper et al., 2018), rather than impermeable bare ice as previously assumed (Arnold et al., 1998). For this reason, it may not be appropriate to

apply principles of supraglacial open-channel flow everywhere on the ice surface, i.e. subsurface flows may be more suitable for describing meltwater transport in the interfluve (hillslope) areas of higher-elevation ice separating meltwater channels. This reality calls for an easy-to-use, straightforward method to partition ice surface into channel vs. non-channel (i.e. interfluve) flow with each experiencing different physical flow processes. The Rescaled Width Function (RWF) is our proposed solution for this partitioning.

We selected RWF over other SUH methods for the following reasons: 1) most SUH methods do not include interfluve (hillslope) transport and consider only the open channel network on water routing (Singh, et al., 2014), whereas RWF includes both hillslope and open-channel flows; 2) RWF is straightforward to implement and couple with remote sensing, requiring only hillslope and open-channel zones as inputs; 3) although RWF is a spatially-lumped model, it can provide catchment-scale meltwater routing velocities, which are crucial for broad-scale understanding of ice surface hydrology. The derived mean open-channel velocity is comparable to field-measured velocities in small supraglacial streams, and the derived hillslope velocity is comparable to simulations of a partially saturated subsurface hydrological model. Therefore, RWF appears to be a simple and useful tool for modeling meltwater routing across broad-scale areas of melting ice.

Additional new text has been added to better discuss the choice to use the RWF relative to other methods, as requested (p. 16, lines 13-31).

2. (“What other morphometrics might be important in influencing water routing in IDCs, and how might the utility of this method vary spatially?”)

Reply: Thanks for this thoughtful comment. From a hydraulic modeling perspective, supraglacial channel width, depth, and stream order all influence meltwater routing in IDCs. However, these parameters are difficult to estimate at a catchment scale. Moreover, we investigated surface meltwater routing from a hydrological modeling perspective and used RWF to estimate spatially-lumped meltwater routing velocities and transport times. As such, other aspects of meltwater channel morphometrics are not included in this study.

Although RWF is a spatially-lumped model, it has already provided catchment-averaged meltwater routing velocities and reasonable moulin hydrographs. These information may be sufficient to build a surface-to-bed meltwater connections at present since subglacial hydrological models are still at their early development stage and require simple moulin inputs. We leave spatially-distributed routing models for future studies because of two reasons: first, these models need more data inputs and parameters (which are difficult to estimate) than RWF; second, we need to determine what additional scientific value would be gained from more complex models.

Additional new text has been added to better discuss the necessity to develop spatially-distributed models based on RWF in future work (p. 17, lines 23-25).

3. (“Additionally, given that forward progress in constraining the hydrological processes of IDCs is limited by field data, it would be useful if the discussion section laid out a set of key priority areas for field work that would allow us to generalize this method beyond the

current catchment.”)

Reply: We suggest that the catchment-averaged meltwater routing velocities (hillslope and open-channel velocities) can be applied to other ungauged IDCs. The derived open-channel velocity matches well with field-measured discharge of small supraglacial streams, while the derived hillslope velocity matches with simulations of a partially saturated subsurface hydrological model. Therefore, it is promising to employ RWF to study surface meltwater routing in a broader-scale area.

Selecting of an IDC for field study is logistically challenging and requires careful planning and design. We selected the Rio Behar catchment by considering surface melt intensity, distance to ice edge, distance to automatic weather stations, catchment size and shape, catchment outlet (moulin) conditions, and safety conditions (Smith et al., 2017). Two types of field measurements will be crucial for better understanding of surface meltwater routing process: supraglacial river discharge and subglacial water pressure. Supraglacial river discharge hydrographs can be used to validate the performance of surface meltwater routing methods, while subglacial water pressure can be used to estimate the hydrological responses of subglacial environments to different supraglacial meltwater inputs (moulin discharge).

Additional new text has been added to better discuss generalization of RWF beyond the current catchment, as requested (p. 18, lines 3-10).

4. (“This paper is situated in a recent proliferation of studies attempting to generate accurate and generalizable approaches to estimating moulin hydrographs. To further emphasize the contribution of this work beyond its methodological scope, the paper would benefit from further considerations of the implications of this study relative to our understanding of the hydrology of the ice sheet (e.g. under what conditions might we expect the distribution of routing between interfluvies and channels to have meaningful impacts on subglacial hydrology, how might this vary in catchments of different sizes, at different elevations, etc..).”)

Reply: This is a great suggestion that is unfortunately a research question. Answering it effectively will require coupling a surface meltwater routing model with a subglacial hydrological model, which is beyond the scope of this study. One path forward would be to use SUH, SRLF, and/or RWF to calculate moulin hydrographs using DEMs of different sources and spatial resolutions, then coupling this output to the Subglacial Hydrology and Kinetic, Transient Interactions (SHaKTI) subglacial hydrology model (Sommers et al., 2018). Doing so would allow derivation of hourly changes in subglacial water pressure in response to different moulin discharge inputs. A logical next step would be to then analyze the potential impact of these varying subglacial water pressures on subglacial hydrologic system evolution and ice flow dynamics. An ultimate objective should be to model the complete surface-to-bed meltwater transfer process by using RCMs to generate surface melt, surface routing to generate moulin discharge hydrographs, and subglacial models to track basal water pressure, subglacial hydrological system evolution, and ice flow.

Attempting these steps is beyond the scope of the current paper, but we now outline them as a Section 6.6 “Future research directions” (p. 18, lines 19-29).

Sommers, A., H. Rajaram, and M. Morlighem (2018), SHAKTI: Subglacial Hydrology and Kinetic, Transient Interactions v1.0, Geosci. Model Dev., 11(7): 2955-2974.

RECOMMENDATION: This paper is well written and employs a clear and meticulous methodology with careful consideration of its limitations. I recommend publication of this work with some comments as outlined above and additional minor considerations that I outline below.

Specific comments:

5. (“Title: The title is not sufficiently descriptive to distinguish the contribution of this paper from prior contributions in this field. Further, I think that ‘internally drained catchments’ somewhat misrepresents the work given that the focus of this paper is derivation of the daily moulin hydrograph for a specific IDC. I strongly suggest rewording the title to emphasize that this contribution is at a more spatially, hydrologically, and geomorphologically precise scale than prior work in this area.”)

Reply: Thanks for this suggestion. We have changed the title into: “A new surface meltwater routing model for use on the Greenland Ice Sheet surface” (p. 1, lines 1-4).

6. (“Abstract, page 1, line 17: Replace ‘it’ with specific term – accurately modelling moulin hydrographs?”)

Reply: “it is” has been replaced with “accurately modelling moulin hydrographs are”, as suggested (p. 1, line 19).

7. (“Introduction, Page 2, line 9: IDCs constrain. . . suggest more specific wording, e.g. : IDC spatial and temporal characteristics and processes constrain. . .”)

Reply: Changed as requested (p. 2, line 12).

8. (“Page 2, line 15: citations for underlying bedrock controls. I suggest citing Lampkin and Vanderberg (2011) who did earlier work on the topic of bedrock controls on supraglacial hydrological features.”)

Reply: The reference to Lampkin and Vanderberg (2011) has been added, as requested (p. 2, line 19).

Lampkin, D. J., and J. VanderBerg (2011), A preliminary investigation of the influence of basal and surface topography on supraglacial lake distribution near Jakobshavn Isbrae, western Greenland, Hydrolo. Process., 25(21): 3347-3355.

9. (“Page 2, Line 29: Clason et al. 2015 did attempt to account for some snowpack retention and runoff delay by factoring in runoff delays due to snowpack retention, although not

specifically delays due to routing – would be worth mentioning.”)

Reply: This point has been added, as suggested (p. 3, lines 2-3).

10. (“Page 3, Line 18: specify that, in this case, the lumped spatial domain is the IDC scale.”)

Reply: “The lumped spatial domain is the moderate IDC scale (~60 km²)” has been added, as suggested (p. 3, line 28).

11. (“Page 3, Line 21: is the 3 m resolution unprecedentedly high? ArcticDEM is 2 m resolution and has been used by Karlstrom and Yang (2016) and King et al. (2016) for flow routing in supraglacial environments. Additionally, Rippin, Pomfret and King (2015) used UAVderived DEMs of 10 cm resolution for derivation of supraglacial channels.”)

Reply: We meant that a high resolution DEM has never been used to simulate surface meltwater routing so it is unprecedentedly high for this particular application. To avoid misleading readers we have now deleted “unprecedented”, as requested (p. 3, line 30).

12. (“3. Data sources Page 4, lines 29 – 32. For full reproducibility, please include method of degradation and spatial filtering algorithm names (e.g. mean filter, median filter, Gaussian filter?).”)

Reply: We used NASA's Open Source Automated Stereogrammetry Software, ASP (Ames Stereo Pipeline), to create high-resolution DEMs using 0.5 m WorldView (WV) images (Smith et al., 2017). We first used the tool “wv_correct” to correct for subpixel camera alignment artifacts in the full-resolution imagery. The second step is to use the mapproject tool in the ASP to project the left and right images onto a lower resolution DEM. We projected on to the GIMP DEM from OHio State and used bicubic interpolation to downsampled WV images from 50 cm to 1 m. Data source section has been shortened as the Reviewer #2 suggested (p. 5, lines 5-7).

13. (“4.3 Unit Hydrograph Page 6, Line 22: move explanation of M’ to line 18, first mention of M’. In this section or in the introduction it would be useful to include a brief discussion of what other SUH methods are available (e.g. Geomorphic Instantaneous Unit Hydrograph) and why they were not employed in this case. Given that the focus of this paper is methodological, it would be useful for other researchers, particularly glaciologists without a familiarity with SUH derivations, to get a broader sense of the range of hydrological approaches that might be used in the context of this work as well as in Smith et al., (2017).”)

Reply: Some other more complex SUH methods have also been proposed for terrestrial hydrology but most of those methods cannot partition physical flow processes either (Singh et al., 2014). For example, the Geomorphic Instantaneous Unit Hydrograph (GIUH) method includes open-channel flow but ignores hillslope flow (Moussa, 2008), which is not suitable for representing meltwater routing on the ice surface. This point has been added to the Introduction section, as requested (p. 3, lines 22-25). See our reply to your comment #1 for

more detail.

14. (“4.5 Rescaled Width Function Page 7, Line 20: can constant flow velocities be assumed for interfluvial and channel zones? It seems that flow in channels is highly dependent on location within the network (Gleason et al., 2016). This is acknowledged and addressed in the limitations, but I would be interested in seeing a breakdown of the structure of the channel network in order to get a sense of the scale over which flow velocities vary. The distribution of total (or mean) channel length by stream order, contributing area, or by channel width would be useful. This could be done as a cumulative distribution, for example, and the effect of the seasonal evolution of the drainage network could be included by showing the drainage network breakdown according to variable A_c values.”)

Reply: Open-channel and interfluvial flow velocities vary spatially in IDCs, as the reviewer pointed out. The constant flow velocities we quantified using Rescaled Width Function (RWF) are “bulk” velocity averaged over the entire IDC. These bulk velocities are useful for characterizing the overall pattern of IDC surface meltwater routing but unfortunately their spatial variations are not derivable using the RWF method. However, Yang et al. (2016) showed supraglacial river width and depth both increase with stream order so we might expect open-channel flow velocities to also increase with stream order based on hydraulic geometric characteristics. Gleason et al. (2016) suggested that supraglacial meltwater channels primarily accommodate greater discharges by increasing velocities. Variable open-channel velocities will lead to different IDC hydrological responses to surface melt and thereby variable UHs will be generated. Several spatially distributed routing methods have been proposed in terrestrial hydrology for this purpose (Melesse and Graham, 2004) and these methods are different from RWF’s constant velocity assumption.

To better clarify this difference between RWF and other routing models, additional new text has been added in the Section 6.4 “Advantages and Limitations of RWF” (p. 16, lines 13-31).

Melesse, A. M., and W. D. Graham (2004), Storm runoff prediction based on a spatially distributed travel time method utilizing remote sensing and GIS, *J. Am. Water Resour. Assoc.*, 40(4): 863-879.

15. (“5.2 Interfluvial and open-channel travel distances Page 9, Line 12: travel distances. I was confused about the travel distance comparison for some time, until it became clear to me that your L_c is in km and your L_h is in m. I suggest for the sake of clarity, put the in-text travel distances in the same units, particularly as Figure 4 is in m for both travel distances. I think it will improve the clarity and readability of this section. Overall for the travel distances section, your findings are that the interfluvial travel distances are orders of magnitude shorter than the channel travel distance, and surely this is the same regardless of the channel initiation threshold you use (as per Table 1). Rather than justifying the difference between your findings for the conservative threshold and Karlstrom et al. (2014) and McGrath’s et al. (2011)’s findings, I would simply state that although your findings for interfluvial travel distances (in particular) vary with initiation area and are closer to prior work at the non-

conservative river detection threshold, the orders of magnitude difference between channel and interfluvial travel time remains effectively unchanged relative to the difference between the two process domains.”)

Reply: We have changed the unit of L_c into m, as requested. In Table I, we used small A_c values on purpose to simulate well-developed supraglacial river networks mapped from satellite imagery but this does not mean that other larger A_c values will yield similar results. For example, if A_c is set to 5000 pixels, supraglacial river network will be poorly developed and the resultant hillslope distance (L_h) increases to the order of 10^2 m. Additional new text has been added to better illustrate this point (p. 8, lines 23-27; p. 9, line 25; p. 37, Table I).

16. (“5.3 Interfluvial and open-channel travel velocities. As per my comment above, I would be interested in seeing some breakdown of the relative dominance of channel of different widths or orders. Assuming you have a mask of channel extents, would it be possible to generate a histogram of river widths in the study area? This would provide some context for comparison between your bulk-catchment v_c and prior work.”)

Reply: RWF is a spatially-lumped meltwater routing model, meaning that a breakdown of spatially explicit channel widths, stream orders, velocities, etc. is not possible within this particular routing model. However, we generated the meltwater channel width histogram of the conservatively mapped supraglacial stream/river networks in the study area as the reviewer suggested (Figure S1). The result shows that most supraglacial meltwater channels are narrower than 4 m and the resultant mean width is 2.5 ± 2.0 m, supporting our conclusion that numerous small supraglacial streams control bulk-catchment v_c . We have added an Appendix section and new Figure S1 to present this additional work, as requested (p. 22, lines 5-12; p. 36, Figure 9).

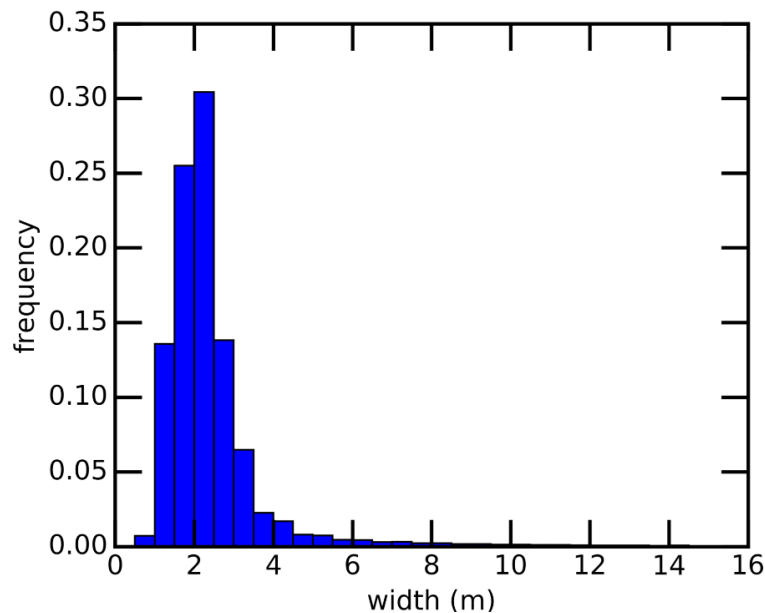


Figure S1. Channel width histogram of conservatively mapped supraglacial stream/river networks in Rio Behar catchment. Most supraglacial meltwater channels are narrower than 4 m with a mean width of 2.5 ± 2.0 m, confirming that numerous small supraglacial streams dominate the bulk-catchment average channel velocity v_c .

17. (“5.5 Moulin hydrograph simulations. Although the SRLF-GIMP hydrograph is different, it does not appear to be ‘significantly’ so. I wonder what the implications of the observable difference are, and whether these implications are significant at scales that affect subglacial channel evolution. Some discussion of the conditions under which this difference in hydrograph simulations might be accentuated would be useful (e.g. small vs. large basins, etc. . .). Or, perhaps including the volume of water would be useful for context, rather than just the RWFUH. Amplified by the total volume of water collected in this catchment, how significant does this offset become in a physical sense?”)

Reply: See our reply to comment 4. This is an outstanding research question for future studies, which could be answered by coupling the RWF routing model with a subglacial hydrological model. Additional new text has been added to Section 6.6 “Future research directions” to explain this (p. 18, lines 19-29).

18. (“6.1 Surface runoff delays on the Greenland Ice Sheet Page 12, Line 28: is the MAR runoff delay a delay due to runoff routing, or a delay in the production of runoff due to melt storage in the snowpack?”)

Reply: To our understanding, the MAR runoff delay is achieved by three empirically calibrated coefficients, without any physical meanings (e.g., runoff routing or snowpack storage). The underlying idea is that meltwater reaches the drainage system quicker when the general surface slope is larger. Specifically, the delay function is:

$$\frac{dW}{dt} = P_w - \frac{W}{t^*}$$

where $t^* = c_1 + c_2 \exp(-c_3 S)$. P_w is “the production of meltwater that does not refreeze, t^* is “the characteristic time-scale for meltwater runoff”, and S is surface slope. Zuo and Oerlemans (1996) determined optimal values for c_1 , c_2 , and c_3 by “optimizing the simulated albedo against the observations” and the resultant values are 1.5, 25, and 140. Lefebvre et al. (2003) updated the coefficients to 0.33, 25, and 140 in order to route meltwater more rapidly. In this study, we show that surface meltwater routing is a crucial physical process but ignored by the RCM models. MAR attempts to impose a delay, but the delay function is purely empirical, with no physical basis, unlike the routing models examined in this study.

19. (“Page 13, Line 6: This is interesting.”)

Reply: Yes, Van As et al. (2017) presented a very interesting way to quantify surface meltwater routing delay at a broad scale, which directly inspired this study.

20. (“6.2 Seasonal evolution of the supraglacial drainage network Page 13, Line 25 – 27: Could these variations in water pressure be due to an evolving sub-glacial network that is better able to transport peak diurnal flow in August? How could we disambiguate these processes?”)

Reply: Subglacial drainage network is best-developed in August so it may indeed also contribute to the observed diurnal variations in subglacial water pressure. Separating this effect from supraglacial delays will require coupling RWF with a subglacial hydrologic model, allowing different supraglacial meltwater inputs to disambiguate the contributions of supraglacial and subglacial processes. Additional new text has been added to explain this (p. 14, lines 11-13).

21. (“Page 14 – line 11: Do you not have in-channel measurements of width and depth with which to derive R ? R should be in units of meters – in which case your R value seems very low (Manning’s n is not dimensionless, although it is often represented that way). Also, is the slope value of the catchment surface, or the channel slope? It should be channel slope if you are using the Manning’s equation for open channel flow.”)

Reply: We only have in-channel measurements of width and depth at one cross-section at the very end of the main-stem supraglacial river. On the IDC scale, the mean hydraulic radius (R) is dominated by small supraglacial streams due to their numerous number. Arnold et al. (1998) used 0.035 m and we think this is a reasonable assumption. For a small supraglacial meltwater channel with width = 0.25 m, depth = 0.05 m, and rectangle shape, the resultant R is 0.035 m. Because we derived slopes from the DEM, they represent ice surface slope rather than channel slope. We used the mean ice surface slope as an approximate for the channel slope because we do not have any *in situ* small channel slope measurements. Additional new text has been added to better explain this (p. 14, line 27; p. 20, lines 18-20).

22. (“6.3 Is interfluvial meltwater dominated by overland flow or subsurface flow? This is a nice discussion of the mechanisms dominating interfluvial water routing.”)

Reply: Thanks. Determination of interfluvial meltwater flow types is crucial for understanding surface meltwater routing. A mechanistic study should be conducted in future to further illustrate the related processes (overland flow, fully saturated subsurface flow, and partially subsurface flow).

23. (“6.4 Limitations. This section provides a good overview of the limitations of the RWF method. However, I would also like to see some mention of the morphometrics that are not addressed by the RWF, such as drainage network complexity (e.g. the distribution of streams of different orders), and channel and interfluvial slope.”)

Reply: Because RWF is a spatially-lumped, process-partitioned meltwater routing model it cannot handle spatially-distributed IDC morphometrics and requires assumption of constant velocities for interfluvial and open-channel flow. This is actually an advantage of RWF because it allows RWF to partition mean catchment-scale interfluvial and open-channel flow velocities and consequently the overall hydrological response of the IDC to surface melt. We agree with the reviewer that the IDC morphometrics (e.g., drainage network complexity and channel and interfluvial slope) should be investigated for building a spatially-distributed

meltwater routing model but due to the “bulk” nature of the RWF model it is beyond the scope of this study. A new section explaining this has been added to the paper (p. 16, lines 13-31).

24. (“Appendix I: R should have units of m (defined as area $[L^2]$ over perimeter $[L]$). Again, I am not clear on how a constant R of 0.035 m and thus a depth of 0.05 m is used in this case. Is this meant to be catchment-averaged? For the SRLF, which is distributed, one would expect R and depth to change with every pixel, no? Some clarification of these assumptions is needed.”)

Reply: See our reply to your comment #21. Arnold et al. (1998) used constant R and spatially varied slope to obtain spatially varied velocities for IDC pixels. Thereby, SRLF assumes small supraglacial streams ($R = 0.035$ m) develop everywhere on the ice surface and does not consider variations of supraglacial stream/river network morphometrics (e.g., width, depth, and Stream order) so it is meant to be catchment-averaged. Additional new text has been added to better explain this (p. 14, line 27; p. 20, lines 18-20).

25. (“Figure 3: according to the text, the WV-1 image was acquired on 18 July, and the UAV image on 20-22 July, therefore the images are not concurrent?”)

Reply: Yes, the WV-1 image and the UAV image are not concurrent. Supraglacial stream/river networks are assumed to have been more or less stable during 18-22 July 2015.

References:

- Gleason, C. J., Smith, L. C., Chu, V. W., Legleiter, C. J., Pitcher, L. H., Overstreet, B. T., Rennermalm, A. K., Forster, R. R. and Yang, K. (2016) ‘Characterizing supraglacial meltwater channel hydraulics on the Greenland Ice Sheet from in situ observations’, *Earth Surface Processes and Landforms*, 41(14), pp. 2111–2122. doi: 10.1002/esp.3977.
- Karlstrom, L. and Yang, K. (2016) ‘Fluvial supraglacial landscape evolution on the Greenland Ice Sheet’, *Geophysical Research Letters*, 43, pp. 2683–2692.
- King, L., Hassan, M. A., Yang, K. and Flowers, G. E. (2016) ‘Flow Routing for Delineating Supraglacial Meltwater Channel Networks’, *Remote Sensing*, 8(988). doi: 10.3390/rs8120988.
- Lampkin, D. J. and Vanderberg, J. (2011) ‘A preliminary investigation of the influence of basal and surface topography on supraglacial lake distribution near Jakobshavn Isbrae, western Greenland’, *Hydrological Processes*, 25(21), pp. 3347–3355. doi: 10.1002/hyp.8170.
- Rippin, D. M., Pomfret, A. and King, N. (2015) ‘High resolution mapping of supraglacial drainage pathways reveals link between micro-channel drainage density, surface roughness and surface reflectance’, *Earth Surface Processes and Landforms*. doi: 10.1002/esp.3719.
- Smith, L. C., Yang, K., Pitcher, L. H., Overstreet, B. T., Chu, V. W., Rennermalm, K., Ryan, J., Cooper, M. G., Gleason, C. J., Tedesco, M., Jeyaratnam, J., van As, D., van den Broeke, M., van de Berg, W. J., Noel, B., Langen, P. L., Cullather, R. I., Zhao, B., Willis, M. J., Hubbard, A., Box, J. E., Jenner, B. A. and Behar, A. E. (2017) ‘Direct measurements of meltwater runoff and retention on the Greenland ice sheet surface’, *Proceedings of the National Academy of Sciences*, 114(50), pp. 1–40. doi: 10.1073/pnas.1707743114.

Reviewer #2

This is a very good paper that makes a solid contribution to our understanding of supraglacial hydrology at the process level. It is well written, provides a nice level of detail and uses a really great dataset. It is a clear example of the scientific advances made possible by the availability of very high resolution satellite data. I found the discussion of interfluvial vs channel flow very interesting and it is this in particular which will be of use to others who are interested in modelling surface hydrology at the broader scale e.g. regional or ice-sheet-wide.

1. ("The major limitation of this paper in this respect is that the scientific findings are somewhat parochial and it is not clear at present how far they can be applied beyond the Rio Behar catchment. I would also have liked to have seen more consideration of whether the results scale in the context of modelling supraglacial hydrology on a grid with resolution of the order of 100 m or so. For example a sensitivity analysis with respect to DEM resolution. I agree with the other reviewer that this paper presents a solid methodological basis for studies in other catchments, and indeed the authors themselves present their study as a starting point for further work at the broader scale. I therefore recommend publication subject to the following, mainly minor, comments being addressed.")

Reply: We respectfully disagree that the study is parochial. Rescaled Width function (RWF) is a flexible, simple-to-use spatially-lumped meltwater routing model that takes an important step forward by distinguishing between flow characteristics in open-channels versus interfluvial. Because open channels and interfluvial are ubiquitous in the bare-ice ablation zone of the western Greenland this conceptual advance should be broadly applicable beyond the Rio Behar catchment on similar bare-ice surfaces of western Greenland. We have compared RWF with other SUH methods, demonstrated the impacts of different moulin inputs on subglacial water pressure, and discussed the necessity to develop spatially-distributed meltwater routing models. See our reply to comment 1-3 of Reviewer #1 for more detail.

It is nontrivial to analyze the impact (sensitivity) of DEM spatial resolution on surface meltwater routing. Crucial ice surface topographic characteristics, such as slope, flow direction, flow length, drainage area, and drainage networks, are scale-dependent. Zhang and Montgomery (1994) illustrated DEM resolution significantly impacts hydrological responses of terrestrial catchment to rainfall, using 2 m, 4 m, 10 m, 30 m, and 90 m DEMs. We suggest that DEM source and catchment geo-morphometry both affect a DEM's capability for simulating meltwater routing on the ice surface. In general, a 100 m or coarser resolution DEM may yield larger offsets in simulating moulin hydrographs compared to a 30 m resolution DEM but the specific offsets need further estimation.

Moreover, high-resolution ArcticDEM (Noh and Howat, 2015, 2017) raises prospects for studying meltwater routing in unprecedented detail and it covers the entire Greenland Ice Sheet at present. The ArcticDEM products are now released at 2 m, 10 m, 32 m, 100 m, 500 m, and 1000 m resolution (Release 7, September 2018). Therefore, we recommend using ArcticDEM products in future meltwater routing studies.

We leave DEM resolution sensitivity for future studies because we focus on RWF in this study. RWF can only be conducted on high-resolution (< 10 m) DEMs because DEM spatial

resolution should not exceed hillslope transport distance; otherwise, hillslope transport distance would be significantly overestimated and the resultant hydrograph would be inappropriate (Hancock et al., 2006). Put another way, coarse-resolution DEMs are unable to differentiate between small channels and interfluvies, which are exactly the two surface-types that RWF partitions. In the future, we plan to use the newly released ArcticDEM products to better illustrate the impact (sensitivity) of DEM spatial resolution on surface meltwater routing and consequently investigate surface meltwater routing in a broad-scale area.

Additional new text has been added to better highlight the advantage of RWF model and DEM resolution's impact on surface meltwater routing (Section 6.6 "Future research directions", p. 18, lines 19-31, p. 19, lines 1-7).

Hancock, G. R., C. Martinez, K. G. Evans, et al. (2006), A comparison of SRTM and high-resolution digital elevation models and their use in catchment geomorphology and hydrology: Australian examples, *Earth Surface Processes and Landforms*, 31(11): 1394-1412.

Zhang, W., and D. R. Montgomery (1994), Digital elevation model grid size, landscape representation, and hydrologic simulations, *Water Resour. Res.*, 30(4): 1019-1028.

2. ("Throughout: Please add spaces between references")

Reply: Spaces have been added between references, as requested (p. 23-27).

3. ("Page 2, line 11: consider adding 'on seasonal and shorter-term timescales'")

Reply: Added as suggested (p. 2, line 15).

4. ("Page 2, Line 16: add a sentence about basal-surface transmission being dependent on ice thickness (Lampkin and van der Berg, 2011).")

Reply: Supraglacial drainage patterns are primarily determined by ice surface topography, which is influenced by variations in bed roughness and slipperiness and the differing transmission of that variability to the ice surface. Additional new text has been added to better explain this, as requested (p. 2, lines 18-20).

5. ("Page 4, section 2: add a sentence acknowledging that this is sub-grid scale with respect to RCMs and ISMs")

Reply: This sentence has been added to Section 2, as requested (p. 4, lines 13-14).

6. ("Page 4, line 15: What are the elevations of the MAR cells used here? How does this compare to the 'real' elevation of the catchment?")

Reply: We clipped MAR grid cells with the remotely sensed catchment boundary, so the MAR

cell area used to calculate runoff is equal to the true spatial extent and elevation of the catchment (p. 4, lines 20-21).

7. ("Figure 1: Overlay the boundaries of the MAR grid cells used in this study.")

Reply: Changed as requested (p. 28, Figure 1).

8. ("Section 3: This section spends too much time repeating Smith et al., 2017. Suggest rolling sections 3 and 4 into one and replacing much of the section 3 text with a table indicating which data comes directly from that paper. This would also help to more clearly outline the novel contribution of this work.")

Reply: We suggest that it may be better to make this paper self-contained (i.e., independent from Smith et al. (2017)). If we only show a data table without further illustrations, it will be difficult for readers to understand Figure 1 and 2. Subsequently, readers may be confused by the descriptions of Unit Hydrograph and Rescaled Width Function, which are directly related to the Data section. However, we agree with the reviewer that Data section repeated Smith et al. (2017) too much so we have shortened this paragraph to more clearly outline the contribution of this work, as suggested (p. 4, lines 15-30; p. 5, lines 1-8).

9. ("Page 4, line 30: 'point clouds' which 'were'")

Reply: Changed as requested (p. 5, line 6).

10. ("Page 4, lines 28-30: Why did you need to produce this concurrent DEM?")

Reply: This concurrent DEM is used to run both RWF and SRLF models.

11. ("Page 5, lines 8-9: 'Dissected' is a strange choice of words. I'm not sure I understand what you mean by it.")

Reply: By "Dissected", we mean supraglacial stream/river networks heavily incised via thermal erosion of underlying ice. We borrow the term from terrestrial geomorphology, which often uses the word "dissected" to describe badlands and other landscapes that are rapidly eroding due to fluvial activity.

12. ("Page 5, line 29: a 'DEM'")

Reply: Changed as requested (p. 6, line 4).

13. ("Page 6, line 1: Does this mean that you do not accumulate water into lakes? Is this justifiable?")

Reply: These small depressions are considered to be either pathway lakes or DEM noise. This

is justifiable, as we can see from the WorldView satellite imagery and the image-mapped supraglacial stream/river network (Figure 1) that surface meltwater produced in the catchment is routed downslope to the catchment outlet (moulin), without accumulating in lakes.

14. (“Page 6, line 3: I don’t understand what A_c is and how it is incorporated into simulations. Could you please explain this better?”)

Reply: A_c indicates the minimum meltwater contributing area required to form a supraglacial headwater stream. If a DEM grid cell exhibits a contributing area larger than A_c , a supraglacial stream will form and thereby the grid cell belongs to the open-channel zone. In contrast, if a DEM grid cell exhibits a contributing area smaller than A_c , supraglacial stream will not form and thereby the grid cell belongs to the hillslope zone. Larger A_c values will yield larger hillslope zones, whereas smaller A_c values will yield larger open-channel zones. Therefore, a series of increasing A_c values can be used to simulate temporal declining of supraglacial stream/river networks and to create different IDC hydrological responses to declining surface melt inputs. Additional new text has been added to better explain this, as requested (p. 8, lines 23-27).

15. (“Page 6, line 24-26: This should probably go into the list of data taken from Smith et al., 2017”)

Reply: This sentence explains the approach to create UH so we suggest that it belongs to the method section. We moved it to the previous paragraph to make the logical flow smoother (p. 6, lines 19-21).

16. (“Page 8, line 24-26: Perhaps include a comment on the impact on ice albedo.”)

Reply: Conservative and non-conservative thresholding are two ways to delineate supraglacial streams/ivers with different confidences. We suggest that ice albedo does not interact with these two thresholds.

17. (“Page 9, line 3: How do you define ‘channel-like’?”)

Reply: By “channel-like”, we mean narrow, dark linear but not well-channelized feature in the ice surface image. This point has now been better explained (p. 9, line 15).

18. (“Page 9, lines 6-9: Could you use these data to develop a better channel/non-channel classification? From figure 3 it seems to me that the ‘conservative’ map agrees better with the UAV image.”)

Reply: Yes, 0.3 m UAV images can be used to create a higher resolution supraglacial stream/river map. However, the spatial coverage of our UAV images is smaller than that of WorldView satellite images and three UAV image strips obtained from three days would be

needed to cover the Rio Behar Catchment. For consistency, we therefore used the WorldView image to map supraglacial streams/ivers at 0.5 m spatial resolution. The conservative map represents the relatively large supraglacial rivers well so it may visually appear to agree better with the UAV image. However, numerous smaller supraglacial streams among those large rivers were not delineated. This is exactly the reason why both conservative and non-conservative thresholds are used to constrain the real distribution of supraglacial stream/river networks. This point has now been better explained in the revised manuscript, as requested (p. 9, lines 18-20).

19. (“Page 9, line12: ‘mapped rivers’ and burned WV DEM.”)

Reply: Changed as requested (p. 9, line 24).

20. (“Page 9, line 30: How do you define ‘large’? A threshold width?”)

Reply: We defined large supraglacial rivers as the features that can be identified by moderate-resolution (10 – 30 m) satellites (e.g., Sentinel-2 and Landsat-8), while small supraglacial streams as the features that can only be identified by high-resolution (0.5 – 2.0 m) satellites (e.g., WorldView-1/2/3/4). It is subjective to determine a threshold width but if required, we recommend 10 m. This point has been better explained (p. 10, line 12; p. 22, lines 9-12).

21. (“Page 10, line 4 and Table 1: What is ‘E’? Please explain.”)

Reply: E is Nash-Sutcliffe model efficiency (NSE). E is replaced with NSE to for clarity (p. 10, line 17).

22. (“Page 10, lines 8 and 9: I think this is fairly obvious. Suggest rephrase to ‘This finding confirms’”)

Reply: Changed as requested (p. 10, line 21).

23. (“Page 10, section 5.4: What is the ‘time to peak’ in your catchment? Did you look at this? If not, why not?”)

Reply: We have reported the “time to peak” in the Rio Behar catchment (~ 6 hours) in Smith et al. (2017). In this study, we reported total supraglacial travel time rather than time to peak. We use this sentence to better distinguish these two related but different parameters.

24. (“Page 11, lines 3 and 4: I think this is significant for broader scale studies where use of a WV DEM is impractical. What about grids of the order of 100 m?”)

Reply: 100 m or coarser resolution DEM will yield larger offsets in simulating moulin hydrographs compared to 30 m resolution DEM. They will also fail to distinguish between

fine-scale supraglacial streams versus interfluves, the main process-level distinction offered by the RWF routing model. See our reply to comment #1 for more detail (p. 18, lines 30-31; p. 19, lines 1-7).

25. (“Page 11, line 8: Have you tried modifying your SRLF routine to include interfluve flow?”)

Reply: SRLF assumes the entire ice surface behaves like a supraglacial meltwater channel, and therefore Manning’s open-channel flow equation is used to route surface meltwater downslope the bare ice surface to catchment outlet. Therefore, interfluve flow is not included in SRLF. To include interfluve flow, the first step is to partition interfluve and open-channel zones, which is not implemented by SRLF either. If we partition interfluve and open-channel zones and calculate spatially varied velocities for the two zones, we basically create a new spatially-distributed meltwater routing model that is no longer SRLF. See our reply to the first comment of Reviewer 1 for more detail (p. 16, lines 13-31; p. 17, lines 23-25).

26. (“Page 12, line 1: Also earlier in the melt season I expect, i.e. before your study period starts.”)

Reply: During early melt season, snowpack covers the ice surface and a different method is required to route meltwater within and downslope snowpack. Arnold et al (1998) handled this process but this study only focuses on meltwater routing on bare ice surface.

27. (“Page 12, line 14: Delete repeated ‘IDC’”)

Reply: Deleted as requested (p. 12, line 25).

28. (“Page 13, lines 12-14: How? Would you need proglacial discharge measurements for each catchment?”)

Reply: We can apply optimal hillslope and open-channel velocities calibrated for the Rio Behar catchment to generate RWF Unit Hydrograph (RWFUH) for other ungauged IDCs. Consequently, moulin discharge hydrograph for each IDC can be estimated by convolving surface melt with RWFUH and the surface routing delays can be calculated from the output moulin hydrographs. These delays can then be integrated into the corresponding RCM grid cells and thus better parameterize surface runoff in RCM simulations. Additional new text has been added to better explain this, as requested (p. 16, lines 24-31).

29. (“Page 15, line 7: Is it possible to characterise surface conditions using your satellite images or would an in-situ investigation be necessary?”)

Reply: We believe that in-situ investigation is necessary to characterize interfluve conditions. Cooper et al. (2018) analyzed the density and hydrological properties of bare, ablating ice away from open channels, by drilling holes into wet bare ice and measuring the subsurface porosity and water infilling rate, properties that cannot be measured from remote sensing.

Satellite images are certainly useful for providing preliminary observations for ice surface conditions. For example, Smith et al. (2017) partitioned bare ice and snowpack zones using high-resolution satellite imagery and Ryan et al. (2018) investigated ice surface albedo, surface impurities, and cryoconite holes using higher-resolution UAV images. That said, we are unaware of any remote sensing solution to confirm presence/absence of saturated subsurface weathering crust and its hydraulic conductivity, so field measurements remain essential at present.

We have added a new section “6.5 Field site and observation recommendation” to explain how to select field sites and which observations are primarily important for better quantifying surface meltwater routing (p. 18, lines 3-18).

Cooper, M. G., L. C. Smith, A. K. Rennermalm, et al. (2018), Meltwater storage in low-density near-surface bare ice in the Greenland ice sheet ablation zone, *Cryosph.*, 12: 955-970.

Ryan, J. C., A. Hubbard, M. Stibal, et al. (2018), Dark zone of the Greenland Ice Sheet controlled by distributed biologically-active impurities, *Nat. Commun.*, 9(1): 1065.

Smith, L. C., K. Yang, L. H. Pitcher, et al. (2017), Direct measurements of meltwater runoff on the Greenland ice sheet surface, *Proc. Natl. Acad. Sci.*, 114(50): E10622-E10631.

30. (“Figure 1: Explicitly say that the moulin is under the black star.”)

Reply: Changed as requested (p. 28, Figure 1).

Thank you for considering this manuscript for publication in **The Cryosphere**. If we may provide any additional information about the dataset or analysis, please do not hesitate to contact us via the lead author at kangyang@nju.edu.cn.

Respectfully submitted,

Kang Yang
Associate Professor
School of Geography and Ocean Science
Nanjing University

A new surface meltwater routing model for use on the Greenland Ice Sheet surface

Supraglacial meltwater routing through internally drained catchments on the Greenland Ice Sheet surface

5 Kang Yang^{1,2,3}, Laurence C. Smith⁴, Leif Karlstrom⁵, Matthew G. Cooper⁴, Marco Tedesco⁶, Dirk van As⁷, Xiao Cheng^{2,8}, Zhuoqi Chen^{2,8}, Manchun Li^{1,3}

¹School of Geography and Ocean Science, Nanjing University, Nanjing 210023, China

²Joint Center for Global Change Studies, Beijing 100875, China

³Jiangsu Provincial Key Laboratory of Geographic Information Science and Technology, Nanjing 210023, China

10 ⁴Department of Geography, University of California, Los Angeles, California 90095, USA

⁵Department of Earth Sciences, University of Oregon, Eugene, Oregon 97403, USA

⁶Lamont-Doherty Earth Observatory, Columbia University, Palisades, New York 10964 USA

⁷Geological Survey of Denmark and Greenland, Øster Voldgade 10, 1350 Copenhagen, Denmark

15 ⁸State Key Laboratory of Remote Sensing Science, College of Global Change and Earth System Science, Beijing Normal University, Beijing 100875, China

Correspondence to: Kang Yang (kangyang@nju.edu.cn)

Abstract. Large volumes of surface meltwater are routed through supraglacial internally drained catchments (IDCs) on the Greenland Ice Sheet surface each summer. Because surface routing impacts the timing and discharge of meltwater entering the ice sheet through moulins, accurately modelling moulin hydrographs are it is crucial for correctly coupling surface energy and mass balance models with subglacial hydrology and ice dynamics. Yet surface routing of meltwater on ice sheets remains a poorly understood physical process. We use high-resolution (0.5 m) satellite imagery and a derivative high-resolution (3.0 m) digital elevation model to partition the runoff-contributing area of Rio Behar catchment, a moderate-sized (~63 km²) mid-elevation (1,207-1,381 m) IDC on the southwestern Greenland ablation zone, into meltwater open-channels (supraglacial streams and rivers) and interfluves (small upland areas draining to surface channels, also called “hillslopes” in terrestrial geomorphology). A simultaneous in-situ moulin discharge hydrograph was previously acquired for this catchment in July 2015. By combining the in-situ discharge measurements with remote sensing and classic hydrological theory, we determine mean meltwater routing velocities through open-channels and interfluves within the catchment. Two traditional terrestrial hydrology surface routing models, the unit hydrograph and rescaled width function, are applied and also compared with a surface routing and lake filling model. We conclude: 1) Surface meltwater is routed by slow interfluve flow (~10⁻³ – 10⁻⁴ m/s) and fast open-channel flow (~10⁻¹ m/s); 2) The slow interfluve velocities are physically consistent with shallow, unsaturated subsurface porous media flow (~10⁻⁴ – 10⁻⁵ m/s) more than overland sheet flow (~10⁻² m/s); 3) The open-channel velocities yield mean Manning’s roughness coefficient (*n*) values of ~0.03 – 0.05 averaged across the Rio Behar supraglacial stream/river network; 4) Interfluve and open-channel flow travel distances have mean length scales of ~10⁰ –

10¹ m and ~10³ m respectively; 5) Seasonal evolution of supraglacial stream/river density will alter these length scales and the proportion of interfluves vs. open-channels, and thus the magnitude and timing of meltwater discharge hydrograph received at the outlet moulin. This phenomenon may explain seasonal subglacial water pressure variations measured in a borehole ~20 km away. In general, we conclude that in addition to fast open-channel transport through supraglacial streams and rivers, slow interfluve processes must also be considered in ice sheet surface meltwater routing models. Interfluves are characterized by slow overland and/or shallow subsurface flow, and it appears that shallow unsaturated porous-media flow occurs even in the bare-ice ablation zone. Together, both interfluves and open-channels combine to modulate the timing and discharge of meltwater reaching IDC outlet moulins, prior to further modification by en- and sub-glacial processes.

1 Introduction

10 Supraglacial internally drained catchments (IDCs) are hydrologic units on the Greenland Ice Sheet (GrIS) surface that collect and drain surface meltwater through supraglacial stream/river networks to terminal moulins or lakes (Thomsen et al., 1989; Yang and Smith, 2016). IDCs spatial and temporal characteristics and processes constrain the location, discharge, lag times, and total volume of surface meltwater penetrating into the ice sheet via moulins (Banwell et al., 2013; Yang and Smith, 2016; Smith et al., 2017), which in turn influences the timing of surface mass loss, subglacial hydrologic system evolution, and ice flow dynamics on seasonal and shorter-term timescales (Zwally et al., 2002; Sole et al., 2011; Banwell et al., 2013; Andrews et al., 2014; Arnold et al., 2014; Clason et al., 2015; Smith et al., 2015; Banwell et al., 2016).

Previous studies have shown that planform IDC locations and shapes are largely induced by underlying bedrock controls on ice surface morphology, which is influenced by variations in bed roughness and slipperiness and the differing transmission of that variability to the ice surface (Lampkin and VanderBerg, 2011; Karlstrom and Yang, 2016; Crozier et al., 2018; Ignéczi et al., 2018), ~~and have~~ IDC areas that generally increase with elevation due to lower moulin densities at high elevations (Poinar et al., 2015; Yang and Smith, 2016). As a result, high-elevation IDCs can drain non-trivial volumes of meltwater into the ice sheet even where overall melt rates are low (Yang and Smith, 2016; Smith et al., 2017). Analysis of satellite imagery suggests that by mid-July, over 95% of IDCs in the southwest GrIS drain meltwater into moulins rather than lakes (Fitzpatrick et al., 2014; Smith et al., 2015). The variable sizes and shapes of IDCs influence the timing and magnitude of peak meltwater injection into the ice sheet through these moulins (Smith et al., 2017).

Few studies have examined meltwater surface routing processes through IDCs on the Greenland Ice Sheet ablation zone surface. Therefore, our ability to simulate IDC moulin hydrographs and, by extension, realistic surface-to-bed connections, remains limited. Most studies to date have used surface melt rates simulated by Regional Climate Models (RCMs) to calculate runoff (hereafter called “moulin discharge”) assumed to flow to the IDC’s terminal outlet moulin, but without explicit treatment of surface meltwater routing processes and associated time lags (Smith et al., 2017). This can introduce large uncertainty in the timing and magnitudes of meltwater injection into the ice sheet, impacting the accuracy of subglacial hydrology and dynamical ice flow simulations.

Previous studies have addressed this problem in different ways. Clason et al. (2015) used a single-flow direction algorithm to route surface meltwater across the ice surface and accounted for factoring in runoff delays due to snowpack retention; Arnold et al. (1998) developed a distributed surface routing and lake filling (SRLF) model to simulate moulin discharge. The SRLF was designed for snow- or bare ice-covered IDCs, and has since been used to simulate the effects of up-glacier snowline retreat on meltwater routing (Willis et al., 2002), drive subglacial hydrologic system evolution (Banwell et al., 2013; Banwell et al., 2016), fill supraglacial lakes (Banwell et al., 2012; Arnold et al., 2014), and illustrate ice flow patterns (de Fleurian et al., 2016). Leeson et al. (2012) developed a similar surface meltwater routing model based on Manning's equation for open-channel flow and Darcy's law for subsurface flow through a porous medium to simulate lake evolution on the GrIS.

As with terrestrial hydrologic models, supraglacial meltwater routing models are highly sensitive to the choices of surface routing scheme, some poorly quantified parameters (e.g., Manning's roughness coefficient n , mean flow velocity, lag time-to-peak, near-surface permeability) and input data (e.g., RCM model output, Automated Weather Stations). Karlstrom et al. (2014) measured and modeled subsurface porous flow in weathered ice to infer near-surface permeability and found it to be considerably smaller than commonly assumed parameterizations. Gleason et al. (2016) measured hydraulic geometries (width, depth, velocity, slope, Manning's roughness coefficient n , etc.) of nine supraglacial meltwater channels on the southwest GrIS and found n , in particular, to be variable (0.009 – 0.154). Smith et al. (2017) measured a 72-hour *in situ* terminal outlet moulin hydrograph for Rio Behar catchment, a moderately large instrumented IDC (~63 km²). These data were used to empirically calibrate a simple surface meltwater routing model, the Snyder Synthetic Unit Hydrograph (SUH) for broader application across 799 surrounding IDCs remotely sensed across the GrIS ablation zone (Yang and Smith, 2016). However, SUH is a highly "lumped" routing model meaning it does not distinguish between different physical flow processes path within a catchment (Singh et al., 2014), and thereby cannot differentiate between different meltwater routing processes. Some other more complex SUH methods have also been proposed for terrestrial hydrology but most of those methods cannot partition physical flow processes either (Singh et al., 2014). For example, the Geomorphic Instantaneous Unit Hydrograph (GIUH) method only focuses on open-channel flow but ignores hillslope flow (Moussa, 2008), which is not suitable for representing meltwater routing on the ice surface.

This study presents a spatially-lumped, process-partitioned meltwater routing model to investigate surface meltwater routing parameters (meltwater travel distance, velocity, and time) in Rio Behar catchment, using the *in situ* moulin hydrograph of Smith et al. (2017) for calibration. The lumped spatial domain is the moderate IDC scale (~60 km²). Two traditional terrestrial hydrograph analysis tools, the Unit Hydrograph (UH) and Rescaled Width Function (RWF), are used to characterize IDC meltwater routing at an ~~unprecedented~~ high spatial resolution (3 m) afforded using high-resolution remotely sensed digital elevation model (DEM) acquired simultaneously with the *in situ* measurements by the WorldView-1 satellite. RWF offers particular advantages over SUH because it can partition between two different types of flow path (interfluvial vs. open-channel), and quantify their respective mean (or "bulk") meltwater travel velocities within the catchment. The performance of our RWF model is also compared with SRLF to better estimate the performance of RWF and to assess

two different routing approaches. The resultant travel distance, velocity, and time are used to characterize two physically different meltwater routing processes on the ice surface, and the implications of seasonal routing evolutions are discussed. We concluded that a calibrated, high-resolution RWF surface routing model offers good utility for obtaining important meltwater routing parameters and modeling IDC outlet moulin discharge hydrographs on the GrIS bare ice ablation zone.

5 2. Study area

Our study area is the Rio Behar catchment (Smith et al., 2017), a moderate sized supraglacial IDC on the southwest GrIS surface (Fig. 1). It is located in the upper ablation zone, spanning 1207 – 1381 m a.s.l., near the long-term equilibrium line altitude (~1550 m a.s.l.) of this area (van de Wal et al., 2015). In July 2015, the remotely sensed area of the Rio Behar catchment was 63.1 km² and the mainstem length of its trunk supraglacial river was 13.8 km (Smith et al., 2017). Visual analysis of multi-temporal high-resolution satellite and UAV (drone) images shows that the supraglacial stream/river channel network was highly developed in Rio Behar catchment by 21-23 July 2015, when 93.5% of the surface was bare ice. A detailed description of the Rio Behar catchment and remotely sensed imagery, DEM, and catchment map is provided in Smith et al. (2017). Notably, the IDC exhibits sub-grid scale with respect to RCMs and Ice Sheet Models (ISMs) and is considered dominating surface meltwater routing process on the southwest GrIS surface (Yang and Smith, 2016).

15 3. Data sources

For 72 continuous hours (11:00AM 21 July to 10:00AM 23 July 2015) measurements of meltwater discharge exiting Rio Behar catchment were collected using an Acoustic Doppler Current Profiler (ADCP) in the mainstem supraglacial river, ~~about 300 m upstream of its terminal outlet moulin~~ (Smith et al., 2017). Hourly simulations of GrIS meltwater production M over the study period were generated using the MAR (Modèle Atmosphérique Régionale) 3.6 RCM. ~~The MAR 3.6 model is a coupled atmosphere snow regional climate model with 20 km native horizontal resolution~~ (Fettweis et al., 2013). The 20 km MAR grid cells were reprojected to a common 5 km posting and map projection using nearest neighbour resampling. Catchment-mean hourly melt [mm/h] was obtained by clipping MAR grid cells with the remotely sensed Rio Behar boundary (Smith et al., 2017) and summing their corresponding melt values (Fig. 2) , and multiplied by the measured runoff coefficient for the catchment (0.69) to yield units of effective melt M' (Smith et al., 2017).

Two catalogs of stereo WorldView-1 (WV1) panchromatic images (spatial resolution 0.5 m) acquired on 18 July 2015 ~~These images were tasked through the Polar Geospatial Center (PGC) and were ortho-rectified based on the satellite positioning model (Shean et al., 2016). These WV1 images~~ were used for detailed mapping of supraglacial hydrologic features (rivers, lakes, and moulins) (Smith et al., 2017). A fixed-wing UAV (Ryan et al., 2015) acquired aerial camera imagery (RGB bands) over the Rio Behar catchment from 20-22 July 2015. ~~These camera images were processed with Agisoft PhotoScan Pro® to produce an ortho-mosaic with 30 cm spatial resolution (Smith et al., 2017). Due to the relatively~~

~~small changes observed on the ice surface from July 18 to 23, the UAV image mosaic is considered to be comparable or superior to the panchromatic WV1 image and~~ was used to validate the accuracy of supraglacial stream/river delineations derived from the WV1 image.

A concurrent high-resolution (3 m) DEM was derived from these WV1 stereo images using the open source Ames Stereo Pipeline (ASP) toolkit methods (Shean et al., 2016). ~~Prior to processing, we degraded the panchromatic WV1 images to 1 m resolution to aid the speed of DEM production. The ASP toolkit outputs point clouds were spatially filtered to produce a 3 m posting DEM.~~ We used the 30 m GIMP (Greenland Ice Mapping Project) DEM v2 (Howat et al., 2014) for comparison with WV1 DEM.

4. Methods

4.1 Remote sensing of Rio Behar supraglacial river network

A supraglacial stream/river network integrates the hydrologic response of an IDC to surface melt from outside the supraglacial channel system (e.g., the “hillslope” in terrestrial hydrology (D’Odorico and Rigon, 2003)) and open-channel flow (Montgomery and Foufoula-Georgiou, 1993). By late July the ice surface of the GrIS ablation zone becomes heavily dissected with very high drainage density (Smith et al., 2015; Yang et al., 2017) and very short distances between open-channels. The term “interfluvium” is borrowed from terrestrial fluvial geomorphology and refers to small areas of dissected terrain that slope toward rills or gullies. Interfluviums are commonly referred to using the more general term “hillslope”, however in terrestrial geomorphology hillslopes can also refer to much large features whereas interfluviums are a narrower term used for small upland areas with short runoff distances, typically found on heavily dissected surfaces. It is thus the more appropriate term for use on the ice sheet owing to the high observed stream density and correspondingly short distances between supraglacial open channels. Moreover, on the ice surface, there is no analog of soil creep, which is an important process in terrestrial hillslope geomorphology (Montgomery and Dietrich, 1989; Montgomery and Dietrich, 1992). For these reasons we recommend use of the narrower term “interfluvium” instead of the general term of “hillslope”, although the ~~theoretical and~~ mathematical treatments are similar ~~identical~~ for both.

We delineated actively flowing supraglacial streams/ivers from the 0.5 m panchromatic WV1 image, following the automatic detection method of Yang et al. (2017) and Smith et al. (2017). The concurrent UAV image was used to validate the ability of this 0.5 m WV1 image to capture small streams. Two detection thresholds, one conservative (higher) and one non-conservative (lower) with values of 40 and 5 (out of 255), respectively, were applied separately to create two meltwater masks following Gabor-filtering and path-opening processing of the WV1 image (Yang et al., 2017). The conservative threshold extracted linear features that are confidently classified as open-flow channels with clear channel banks and with high spectral contrast from the surrounding ice (Smith et al., 2017), while the non-conservative threshold extracted all the channel-like features in the image (Yang et al., 2015a). The two resultant river masks therefore represent upper and lower

limits for the true distribution of the open-channel supraglacial stream/river network that was actively flowing on Rio Behar catchment when the in situ hydrograph was collected.

4.2 High-resolution DEM processing

Extracting an IDC supraglacial stream/river network from a DEM requires assignment of a prescribed location for the catchment outlet (sink). For this study, the topographic depression containing the known location of the terminal outlet moulin was used as the sink; all other small depressions were filled as per Karlstrom and Yang (2016). This partially filled DEM was then used to calculate flow directions and a downstream flow contributing area raster (Karlstrom and Yang, 2016). Finally, a global meltwater contributing area (A_c) threshold was used to simulate ice surface drainage networks. In practice, if A_c is set too large (small), modeled drainage networks will underestimate (overestimate) real-world channel travel distances, and overestimate (underestimate) actual interfluve travel distances (Montgomery and Foufoula-Georgiou, 1993; Yang and Smith, 2016). Therefore, by deliberately varying this parameter we are able to simulate the seasonal evolution of the supraglacial stream/river network, which tends to have lowest drainage density early and late in the melt season (Yang et al., 2015b; King et al., 2016; Yang et al., 2017). This study used a DEM stream burning technique to force the DEM to produce a reliable actively flowing river network (Lindsay, 2016). To burn the WV DEM, elevations of DEM raster pixels that are spatially coincident with our remotely sensed supraglacial map were lowered (“burned”) by 1.0 m, thereby forcing routed flow to pass through these accurately mapped supraglacial stream/river channels.

4.3 Unit Hydrograph

The unit hydrograph (UH) is a transfer function used to simulate the observed hydrograph (Q) at a catchment outlet for a unit input of water supply (e.g. 1 mm, 1 cm, etc.) applied uniformly across the catchment (Dingman, 2015). Effective M' is the fraction of total MAR melt production M that is transported all the way to the terminal outlet moulin, i.e. the remainder after multiplying by the field measured runoff coefficient (0.69) (Smith et al., 2017). A meteorological dataset M' is used as input to the transfer function, and the resulting simulation is called the “direct hydrograph” (as distinguished from the observed hydrograph). The UH was developed for terrestrial hydrologic applications where precipitation (rain or snow) are the dominant hydrologic inputs (Singh et al., 2014), but is well suited for adaptation on ice sheets by substituting measured or modeled water equivalent from ice melt (Smith et al., 2017), as ice melt is the dominant hydrological input to IDCs in southwest GrIS. Rainfall occasionally occurs during summer in our study area (Van As et al., 2017) but none occurred during our study period.

This allows MAR effective melt (M') to be used as the input data for simulating (routing) the direct hydrograph at the IDC terminal outlet moulin as $Q = M' * \text{UH}$, where $*$ is a convolution operator (Dingman, 2015). ~~Effective M' is the fraction of total MAR melt production M that is transported all the way to the terminal outlet moulin, i.e. the remainder after multiplying by the field measured runoff coefficient (0.69) (Smith et al., 2017).~~ Smith et al. (2017) used the Collins’ method

(Collins, 1939) to create a UH specific to the Rio Behar catchment (here called “MAR UH”), using MAR-produced M' and ADCP-measured Q to calibrate the UH.

In the present study, we also derive other UH transfer functions, which can be built from a satellite image or DEM. To do this, the travel time (t) for each pixel within the IDC is required. Travel time represents the time needed for water to flow from each pixel to the catchment outlet, and the hourly-binned histogram of this travel time raster thus corresponds to a one-hour UH (Liu et al., 2003). Travel time t can be estimated as $t = L/v$, where L is meltwater flow distance and v is flow velocity. Flow distance L can be calculated from DEMs by assuming that meltwater flows from one pixel to the adjacent pixel having the steepest slope (Karlstrom and Yang, 2016).

4.4 Surface routing and lake filling (SRLF) model

SRLF is a distributed, physically based model proposed by Arnold et al. (1998). Model input requirements include DEM elevations and a time series of meteorological forcing data. The model has been widely used for studies of surface meltwater routing in the GrIS ablation zone (Willis et al., 2002; Banwell et al., 2012; Banwell et al., 2013; Arnold et al., 2014; Banwell et al., 2016; de Fleurian et al., 2016). The SRLF uses Darcy’s law to route meltwater flow through snow, and Manning’s equation to route meltwater flow over bare ice surfaces. The present study focuses exclusively on the latter, because satellite and UAV mapping revealed the surface of Rio Behar catchment to be virtually all bare ice during the observational period (Smith et al., 2017).

SRLF can be used to calculate meltwater travel time and thus to create UH. In accordance with Arnold et al. (1998), we calculated a meltwater flow velocity (v) for each pixel in the Rio Behar catchment (see Appendix I). To compute meltwater travel time, a cost surface was created as $1/v$, which was then used as one input raster and flow direction raster was used as another input to determine specific flow paths. The output raster gives travel time for each pixel. The SRLF UH was created by hourly binning the histogram of this travel time raster.

4.5 Rescaled Width Function (RWF)

The rescaled width function (RWF) is a conceptual runoff routing model that represents the total flow distance (L) in a catchment as a combination of an interfluvial (hillslope in terrestrial settings) flow distance (L_h) and a channel flow distance (L_c), i.e., $L = L_h + L_c$. The RWF is an improved version of the width function (WF). WF does not represent interfluvial transport and therefore cannot be used for meltwater routing where interfluvial flow is important (see Appendix II). If constant flow velocities are assumed for interfluvial (v_h) and channel (v_c) zones, the travel time (t) for each pixel is the sum of interfluvial travel time (t_h) and channel travel time (t_c) (Di Lazzaro, 2009). Consequently, catchment UH can be derived from the travel time, which is renamed the RWFUH (Singh et al., 2014).

Determination of v_h and v_c is challenging because water flow velocities are difficult to measure on a catchment scale, especially for interfluvial zones (Moussa, 2008). Although water flow velocities can be predicted theoretically for simple porous flow (Karlstrom et al., 2014) and our more general derivation in Appendix III, the field-measured IDC moulin hydrograph provides a good opportunity to directly calibrate v_h and v_c for a real-world melting ice sheet surface. To achieve this, different combinations of v_h and v_c were used to create RWFUHs. These RWFUHs were then used to simulate direct hydrographs at the IDC terminal outlet moulin for comparison with the corresponding in-situ moulin hydrograph. To evaluate performance between the simulated vs. observed moulin hydrograph, we used the Nash-Sutcliffe model efficiency (*NSE*) cost function (Nash and Sutcliffe, 1970). The *NSE* was calculated for each RWFUH and compared to the field-measured moulin hydrograph and the “optimal” v_h and v_c defined as the combination that maximize the *NSE*.

4.6 Seasonal evolution of the supraglacial stream/river network

By late July, shortwave radiation and air temperatures decline and meltwater production within Rio Behar catchment also declines (Smith et al., 2017). In this study, we assume that low-order streams (i.e., very small tributaries as per Yang et al. (2016)) stop flowing by late July (Yang et al., 2017), higher-order streams/ivers stop flowing by mid-August, and only very large, high-order rivers flow into late August, an assumption supported by remotely sensed supraglacial stream/river maps in Smith et al. (2015) and Yang and Smith (2016). In late July when the supraglacial drainage density is high, fast open-channel transport contributes heavily to meltwater flow routing exiting the IDC. As the supraglacial river network declines and drainage density decreases, interfluvial zones expand and contribute more surface area to overland and/or porous media transport process to IDC flow routing.

To test this idea, we simulated a temporal evolution of the supraglacial stream/river networks within the Rio Behar IDC after late July to characterize the impact of drainage density decline on the RWFUH hydrograph. This test consisted of defining a series of A_c thresholds (i.e., 250, 500, 1000, 2500, and 5000 pixels) that were used to create artificial supraglacial drainage networks from WorldView DEMs. A_c indicates the minimum meltwater contributing area required to form a supraglacial headwater stream. If a DEM grid cell exhibits a contributing area larger than A_c , a supraglacial stream will form and thereby the grid cell belongs to the open-channel zone. In contrast, if a DEM grid cell exhibits a contributing area smaller than A_c , supraglacial stream will not form and thereby the grid cell belongs to the hillslope zone. Larger A_c values will yield larger hillslope zones, whereas smaller A_c values will yield larger open-channel zones. The minimum A_c (250 pixels) was used to simulate a well-developed supraglacial stream/river network, while the maximum A_c (5000 pixels) was used to simulate a poorly-developed stream/river network. Variable A_c values were used to simulate dynamic supraglacial stream/river networks and each A_c value was assumed to last for one week. This sequence of A_c thresholds reasonably mimics the seasonal contraction of the supraglacial stream/river networks after its maximum development in late July (Smith et al., 2015). The resultant drainage networks were then used to calculate moulin discharge (i.e., the direct hydrograph) based

on optimal open-channel and hillslope velocities calibrated from RWFUH, to demonstrate the influence of seasonal drainage network evolution on the shape and timing of the discharge hydrograph at the IDC terminal outlet moulin.

5. Results

5.1 Supraglacial stream/river mapping

5 In total, 3,381 km of actively flowing supraglacial stream/river lengths were confidently mapped (conservative threshold) within Rio Behar catchment, yielding a drainage density of 53.6 km/km² with water bodies covering 8.2% of the catchment surface. Applying the non-conservative detection threshold, 10,829 km of supraglacial stream/river lengths were mapped, yielding a higher drainage density of 164.3 km/km² with water bodies covering 24.1% of the ice surface. These bounding estimates suggest that 76 – 92% of the ice surface area consisted of interfluvial zones with the remainder as supraglacial ponds, lakes, rivers, and streams.

Four test sites were selected to further illustrate the performance of conservative and non-conservative stream/river channel detections (Fig. 3). Sites 1 through 3 are located near the three main tributaries of the Rio Behar catchment where supraglacial streams/rivers are very well developed. Site 4 is located upstream, within an area where supraglacial streams are relatively sparse. Applying the conservative detection threshold delineated supraglacial streams/rivers clearly identifiable in the WV1 image, but narrower channel-like (dark linear but not well-channelized) features among those streams/rivers were missed. In contrast, the non-conservative threshold captured these small features with the resultant streams/rivers being very well-developed and having higher drainage density. Visual inspection of the 0.3 m UAV images (RGB bands) reveals that supraglacial channels mapped with 0.5 m resolution WV satellite imagery capture nearly all conservative channels that can be discerned in 0.3 m UAV camera imagery (Fig. 3). However, numerous smaller non-conservative supraglacial streams among large supraglacial rivers were not delineated. Therefore, we conclude that automatically mapped streams/rivers accurately estimate the minimum and maximum extents of channel and interfluvial zones in the Rio Behar catchment.

5.2 Interfluvial and open-channel travel distances

Meltwater travel distance rasters were calculated for each data source and processing approach (Table 1). Fig. 4 shows the interfluvial and channel travel distances with conservatively mapped rivers and burned WV DEM. The resultant mean channel travel distance is $7.1 \pm 4.0 \times 10^3$ ~~m~~^m, while the resultant mean interfluvial travel distance is 19.7 ± 30.9 m. This signifies that in Rio Behar catchment during our study period, meltwater travel distances through open channels were ~3 orders of magnitude longer than travel distances through interfluvial zones.

This mean interfluvial distance we estimate for Rio Behar catchment is larger than the 0.5 – 5 m values reported for the Juneau Icefield (Karlstrom et al., 2014), and the 9.0 ± 3.4 m interfluvial distance reported for another low-elevation IDC of southwest GrIS (McGrath et al., 2011). However, their interfluvial distances were calculated as the nearest distance from a

interfluvial point to its adjacent channel rather than following the topographic flow direction calculated from DEMs, as in Karlstrom et al. (2014) and McGrath et al. (2011) (although for small slopes the two approaches should yield similar results). River detection thresholds significantly impact interfluvial distances because higher-density distributed meltwater channels lead to smaller interfluvial distances. If the non-conservative river detection threshold is used, the mean interfluvial distance calculated from our burned WV DEM is 6.7 ± 15.0 m, closer to these previously reported estimates.

5.3 Interfluvial and open-channel travel velocities

The optimal RWF-calibrated mean open-channel velocity v_c is on the order of 10^{-1} m/s, while the optimal mean velocity v_h for interfluvial is on the order of $10^{-3} - 10^{-4}$ m/s (Table 1 and Fig. 5). Both conservative and non-conservative approaches quantify open-channel velocities as $v_c = 0.3 - 0.5$ m/s, which are similar to previous field-measured values of $0.25 - 0.5$ m/s in small supraglacial streams (width < 0.5 m) at the Juneau Icefield (Karlstrom et al., 2014), and 0.35 m/s measured for a small supraglacial stream (0.2 m wide) at the southwest GrIS (Gleason et al., 2016). It is slower than faster velocities ($0.2 - 9.4$ m/s) measured in large (>10 m) supraglacial rivers (Smith et al., 2015; Gleason et al., 2016). The relatively low $v_c = 0.3 - 0.5$ m/s quantified for an entire catchment suggests that small, relatively slow-flowing supraglacial streams which are vastly more numerous than large mainstem supraglacial rivers dominated the mean RWF open-channel velocity which is a “bulk” velocity averaged over the entire IDC (Appendix IV).

The RWF-calibrated optimal interfluvial velocity v_h shows larger variation than v_c . The range of v_h is interpreted as $v_h = 0.2 - 1.5 \times 10^{-3}$ m/s if $NSEE = 0.9$. If $NSEE = 0.925$ is used as the calibration threshold, this optimal v_h range is $0.3 - 1.2 \times 10^{-3}$ m/s. Under the assumption that conservative (non-conservative) rivers over- (under-) estimate interfluvial distance, the non-conservative v_h should be considered as the lower v_h limit, while the conservative v_h as the upper v_h limit (Table 1). Although the specific v_h may vary according to different calibration thresholds, Fig. 5 suggests that v_h is on the order of $10^{-3} - 10^{-4}$ m/s. This finding ~~signifies~~ confirms that meltwater is routed through the Rio Behar catchment by slow interfluvial flow ($\sim 10^{-3} - 10^{-4}$ m/s) followed by fast open-channel flow ($\sim 10^{-1}$ m/s).

5.4 Interfluvial and open-channel travel time

The total supraglacial travel time (i.e., the combination of interfluvial and channel travel time) for our study area and period was found to be ~ 11 hours. This suggests that, on average, a unit of application meltwater across the catchment takes 11 hours to arrive at the terminal outlet moulin. However, this should be distinguished from the “time to peak” which describes the lag time between peak meltwater production and peak runoff entering the IDC terminal outlet moulin (Smith et al., 2017), using real-world inputs of melt production which follow a strongly diurnal cycle. The 11 hours reported here refer to a “unit” response, i.e. the average length of time for an instantaneous pulse of 1 cm of meltwater to drain from the Rio Behar IDC.

The optimal v_h and v_c combinations (which maximize NSE) were used to calculate mean meltwater travel time in interfluvial (t_h) and open-channel (t_c) zones. The resultant mean t_h is ~ 6 hours, while the mean t_c is ~ 5 hours. This result differs

from the results obtained for smaller bare ice catchments ($<2 \text{ km}^2$), in which interfluvial travel primarily controls or even dominates meltwater routing (Arnold et al., 1998; Karlstrom et al., 2014). For small catchments, meltwater channels are short and therefore fast travel time through open-channels is less important than slow travel time in interfluvial zones.

5.5 Moulin hydrograph simulations

5 Unit hydrographs (UHs) were created from the meltwater travel time maps (driven by the optimal v_h and v_c combinations in Table 1), allowing direct hydrographs at the Rio Behar IDC terminal outlet moulin to be simulated. Similarly, the SRLF model was applied to the WV DEM and the GIMP DEM to create UHs as well (Fig. 6), allowing direct comparisons with our RWF-based methods. Two contributing area thresholds ($A_c = 450 \text{ m}^2$ and 90 m^2) were applied to model supraglacial drainage networks with large ($\sim 23 \text{ m}$) and small ($\sim 9 \text{ m}$) interfluvial distances, which were used for comparisons with the
10 conservative and non-conservative image-mapped river networks, respectively (Table 1).

The UHs simulated by four RWF-based approaches, using two burned WV DEMs, and two A_c -based WV DEMs, generally capture the overall shape of the MAR UH (with a duration of 25 hours, see Smith et al. (2017) for more details). All of these four RWF-based UHs smooth the MAR UH, signifying that surface routing of meltwater distributes runoff more uniformly over time (Dingman, 2015). The SRLF-based WV DEM UH also performs reasonably well, although its shape is
15 more irregular, similar to the MAR UH. The UH simulated by the 30 m GIMP DEM is different from all the other UHs in that it distributes all of the input meltwater during the first 13 hours, suggesting that ~~the~~this coarse resolution DEM overly “speeds up” the surface meltwater transport (Fig. 6a).

Both RWF-based and SRLF-based UHs simulate the moulin hydrograph well (Fig. 6b). Except for the GIMP DEM SRLF approach, all the other RWF-based and SRLF-based approaches were able to accurately simulate the peak discharges
20 of the observed moulin hydrographs. These approaches also captured the peak time of the first daily hydrograph, whereas a 2 – 4 hour time lag was obtained for the second daily hydrograph. However, because SRLF lacks slow interfluvial flow, it routes surface meltwater faster than RWF and distributes all of the input meltwater during the first 20 hours (Fig. 6a). Ignoring the slow interfluvial flow affects the performance of SRLF method negatively, yielding an optimal $NSE = 0.8742$, smaller than for the RWF method (Table 1). Moreover, the SRLF-based GIMP DEM hydrograph is considerably different
25 from the observed moulin hydrograph. This suggests that DEMs with a resolution exceeding $\sim 30 \text{ m}$ may fail to accurately capture the velocities and time delays of surface meltwater routing.

5.6 Performance of conventional DEM-based simulations

The two conventional DEM-based simulations (Methods section 4.2), assuming a large and small value of the threshold A_c , yielded similar results as the burned DEM approaches. The supraglacial drainage network simulated by a relatively large A_c
30 (450 m^2 , equivalent to 50 WV DEM pixels) is similar to the conservative image-mapped streams/rivers, whereas the drainage network simulated by the small A_c (90 m^2 , equivalent to 10 WV DEM pixels) is similar to the non-conservative

image-mapped streams/ivers (Table 1). Depending on this choice of A_c threshold and also NSE threshold we find optimal v_h values ranging from $0.3 - 1.2 \times 10^{-3}$ m/s, which is consistent with the optimal range obtained by using the burned WV DEM ($v_h = 0.2 - 1.5 \times 10^{-3}$ m/s). However, v_c shows large variations in optimal values, ranging from 0.4 to 2.0 m/s because DEM-modeled supraglacial drainage networks do not match very well with remotely sensed river networks (Yang et al., 2015b), especially for small supraglacial streams (King et al., 2016). Consequently, the lower value of $A_c = 90$ m² is recommended for use during the peak melting period if a high-resolution remotely sensed supraglacial stream/river map is not available.

5.7 Seasonal evolution of moulin discharge hydrographs

Seasonal changes in the relative proportion of open-channel vs. interfluvial zones substantially alter the timing and magnitude of moulin discharge hydrographs (Fig. 7). If the supraglacial stream/river network is well developed (i.e., has high drainage density) and the interfluvial zone is small, large diurnal variations in moulin discharge are simulated. This finding suggests that under well-developed conditions, open-channel travel is particularly important, similar to results reported for the SRLF model (Banwell et al., 2013).

As the melt season progresses, smaller supraglacial streams dry up and their associated open-channel zone shrinks. Consequently, open-channel travel becomes secondary to interfluvial travel. Under these conditions, meltwater delivery to the englacial system is further attenuated, yielding smaller diurnal variations (Fig.7). This suggests that in absence of a well-developed supraglacial stream/river network, slow interfluvial meltwater transport has a “smoothing” effect on terminal outlet moulin discharge. Similar behavior has been observed or simulated (Arnold et al., 1998; Karlstrom et al., 2014) and is here explicitly modeled using RWF.

6. Discussion

6.1 Surface runoff delays on the Greenland Ice Sheet

The meltwater travel times quantified in this study confirm non-trivial-runoff delays are caused by at least two fluvial meltwater transport processes operating within the Rio Behar catchment. Such delays have previously been considered as insignificant in studies of small ice surface catchments (Karlstrom et al., 2014), ~~or modeled incompletely~~. However, even for the moderate-sized (~63 km²) Rio Behar catchment, supraglacial rivers are long (>10 km long mainstem), meaning meltwater can take several hours to pass through the open-channel network. In much larger IDCs (e.g., ~245 km² reported in Yang and Smith (2016)) IDCs, channel routing delays are even longer. Therefore, the present study reinforces the importance of supraglacial stream/river networks in imparting non-trivial delays on surface meltwater transport as a function of IDC area, shape and stream length (Smith et al., 2017), with a new contribution of considering slow interfluvial flow as well as fast open-channel flow.

In contrast to these prior studies, our results suggest that both interfluve and open-channel processes control the timing and magnitude of meltwater transport on the ice sheet. This finding suggests that slow meltwater passage over short distances on interfluvies is compensated by fast meltwater transport over long distances through open channels, such that interfluve travel time was roughly equal to channel travel time during the time of the 2015 field experiment. It is possible, therefore, that supraglacial stream/river networks may mimic the classic graded river concept (Kesseli, 1941; Mackin, 1948), with the open-channel flow network developing into a sufficient density to convey available water supply generated on bare ice interfluvies.

Left untreated, surface routing delays degrade the utility of using RCM models to estimate inputs of meltwater to the subglacial environment and proglacial zone. Most current RCM models do not provide any surface routing functions to represent transport of runoff over the ice surface to moulins (Van As et al., 2014; Cullather et al., 2016). To the best of our knowledge, MAR is the only RCM model integrating a runoff delay function to distribute runoff over time. This delay function was proposed by Zuo and Oerlemans (1996) and is based on the idea that surface meltwater reaches supraglacial channels sooner where the general ice surface slope is larger. The coefficients in the delay function were calibrated by albedo observations on the ice surface, and Lefebvre et al. (2003) updated the coefficients to route meltwater more quickly. Applying the MAR delay function, the resultant runoff delay for the Rio Behar catchment is 8.6 days based on Zuo and Oerlemans (1996) and 7.5 days based on Lefebvre et al. (2003). In contrast, the runoff delay obtained using RWF in our study is only ~11 hours, much shorter than these lumped delays.

Van As et al. (2017) built a statistically based supraglacial-to-proglacial delay function to optimally match modeled runoff with observed proglacial river discharge measurements collected in the Watson River, near Kangerlussuaq. Applying this delay function, the runoff delay for the entire glacial and pro-glacial system is 3.9 days for meltwater generated in the Rio Behar catchment. Van As et al. (2017) used a 10-hour smoothing per 100-m elevation bin to represent supra-glacial routing delays, comparable to our 11-hour travel delay calculated for the Rio Behar catchment. Because this purely statistical approach of Van As et al. (2017) is calibrated using time series of in situ proglacial discharge measurements rather than formulas applied to DEMs as per Zuo and Oerlemans (1996) and Lefebvre et al. (2003), its close agreement with our RWF routing model lends confidence in its more physically realistic routing scheme. Note that the catchment areas of most IDCs are commonly smaller than one MAR cell (Yang and Smith, 2016; Smith et al., 2017). Therefore, for all but the largest IDCs many of the surface routing delays modeled explicitly here could plausibly be parameterized at the scale of a single large RCM grid cell.

6.2 Seasonal evolution of the supraglacial drainage network

Supraglacial stream/river networks undergo a dramatic seasonal evolution from low- to high- to low-drainage density within just 3-4 months (Lampkin and VanderBerg, 2014; Smith et al., 2015), modifying the shape of IDC terminal outlet moulin hydrographs. Fig. 7 suggests that the moulin hydrograph of the Rio Behar catchment will show small diurnal variations at

beginning and end of a melt season and large diurnal variations during peak melt season. Note that this differs from the classic signal of alpine glaciers, which tend to display a steadily intensifying diurnal cycle throughout the summer as seasonal snowlines climb to higher elevations (Elliston, 1973). Because this seasonal variation may significantly modulate subglacial water pressure and consequently ice flow velocities, this effect warrants further study for other IDCs and using ice dynamical models.

Very interestingly, moulin discharges simulated by Fig. 7 are qualitatively similar to subglacial water pressure variation measured in a borehole ~20 km away from our catchment (67.201° N, 49.289° W; Fig. 7 in Wright et al. (2016)). Although these field-measured subglacial water pressures were obtained during 2011, they show similarly large diurnal variations during late July, smaller diurnal variations during early August, and very small diurnal variations around late August. This may indicate a direct control of seasonally varying surface meltwater routing on subglacial water pressure, which in turn impacts subglacial pathway evolution and ice flow dynamics (Banwell et al., 2013; Wright et al., 2016). Meanwhile, the subglacial drainage network is well developed in late summer (August) (Andrews et al., 2014) so this may also contribute to the small diurnal of subglacial water pressure.

The SRLF model is the most commonly used model for simulating meltwater delivery to moulins and our results suggest it performs well for surface hydrologic conditions similar to those in our study IDC (Banwell et al., 2013; Banwell et al., 2016). More recently, the Synthetic Unit Hydrograph (SUH) has been advanced as a simple way to model the magnitude and timing of moulin runoff based on remotely sensed IDC area, shape, and main-stem stream length (Smith et al., 2017). However, neither SRLF nor SUH considers the seasonal evolution of supraglacial stream/river networks. Owing to its flexibility for partitioning interfluvial and open-channel zones and their changing ratios over time (Mutzner et al., 2016), the RWF provides a good opportunity for improved representation of both interfluvial and open-channel processes, and their evolution over space and time.

The RWF model is calibrated here using a single in situ supraglacial river discharge hydrograph, so the obtained optimal meltwater routing velocities can thus only be confidently attributed to one particular IDC (Rio Behar catchment) during one particular study period (21-23 July 2015). However, other bare-ice IDCs surrounding Rio Behar catchment have similar surface conditions during bare-ice conditions, suggesting some transferability of our results. For example, the calibrated open-channel velocity, i.e., $v_c = 0.3 - 0.5$ m/s, can be used to estimate Manning's n ($n = R^{2/3} S^{1/2} / v_c$); if hydraulic radius R is set to 0.035 m (Arnold et al., 1998) and slope S is set to the mean ice surface slope of the Rio Behar catchment, i.e., 0.024, the resultant n is 0.033 – 0.054, which matches up well with $n = 0.050$ used in Arnold et al. (1998) and $n = 0.035 \pm 0.027$ estimated by Gleason et al. (2016). As such, we suggest-submit that our estimated “bulk” averaged value of $n = 0.03 - 0.05$ is-may be a reasonable estimate for supraglacial streams/ivers under bare ice conditions for use in surface meltwater routing models.

6.3 Is interfluvial meltwater dominated by overland flow or subsurface flow?

Our results suggest that during late July 2015, surface meltwater in Rio Behar catchment was routed by a combination of slow interfluvial flow ($\sim 10^{-3} - 10^{-4}$ m/s) and fast open-channel flow ($\sim 10^{-1}$ m/s). The latter RWF-inferred open-channel flow velocities correspond closely with field measurements (Karlstrom et al., 2014; Gleason et al., 2016), lending confidence that

5 our bulk catchment-averaged values are grounded in a real-world process.

Less clear, however, is the physical process governing interfluvial flow. The rescaled width function (RWF) method we implement assumes that surface meltwater is routed by two distinct flow processes, i.e., open-channel flow and interfluvial flow. The inferred mean interfluvial velocity is $\sim 10^{-3} - 10^{-4}$ m/s, which is 2–3 orders of magnitude smaller than the open-channel velocities ($\sim 10^{-1}$ m/s). While RWF partitioning does not prescribe a physical transport process operating within

10 interfluvies, two likely candidate mechanisms are surface sheet flow and subsurface porous flow.

Sheet flow is overland (over-ice in our case) flow taking the form of a thin, continuous film over relatively smooth surfaces and not concentrated into rills or channels (Mays, 2010). Manning’s kinematic solution is generally used to analyze the sheet flow (Mays, 2010) and the meltwater flow velocity can be calculated as $v_s = f(n, M', S, L_h)$, where n is set to 0.05, $M' = 1.7$ cm is daily effective melt in the Rio Behar catchment, $S = 0.024$ is the average catchment slope, and L_h is set to 1 –

15 100 m. The resultant v_s is $\sim 3 - 8 \times 10^{-2}$ m/s, which is similar to the terrestrial interfluvial velocities (Moussa, 2008; Di Lazzaro, 2009; Singh et al., 2014; Mutzner et al., 2016) but still 1 – 2 orders faster than the ice surface v_h quantified in this study.

This discrepancy suggests that interfluvial transport is most likely controlled by sub-surface meltwater flow, i.e., porous media flow. A fully saturated Darcy’s law has been used in Arnold et al. (1998) and Leeson et al. (2012) (among many others) to describe meltwater routing on firn/snow surfaces. However, to our knowledge, all models of meltwater routing

20 over bare ice assume ice is impermeable and that Darcy’s law is therefore not applicable (Arnold et al., 1998; Banwell et al., 2013; de Fleurian et al., 2016). Field studies do reveal that the bare ice surface of ablating glaciers is often characterized by a porous ice layer termed “weathering crust” (Müller and Keeler, 1969; Fountain and Walder, 1998; Irvine-Fynn et al., 2011; Stevens et al., 2018), and low density well-developed weathering crust has been observed in bare ice of the Rio Behar catchment (Cooper et al., 2018). Our results suggest that in contrast to current practice, principles of porous-media flow may

25 be applied even in the bare-ice ablation zone if conditions of weathering crust and porous low density bare ice are found.

The classic treatment for water transport through porous media is Darcy’s law. Darcy’s velocity (v_d) is defined as $v_d = kS/\phi$, where k is hydraulic conductivity [m/s], S is slope [m/m] and ϕ is weathering crust ice porosity; and hydraulic conductivity k is calculated as $k = K\rho_w g/\mu$, where K is absolute permeability [m^2], ρ_w is water density [kg/m^3], and μ is water viscosity [$\text{kg}/\text{m} \cdot \text{s}$] (Arnold et al., 1998; Leeson et al., 2012). We followed Arnold et al. (1998) to set $\mu = 1.8 \times$

30 10^{-3} $\text{kg}/\text{m} \cdot \text{s}$ and Karlstrom et al. (2014) to set $\phi = 0.1$ for weathering crust ice. Slope S is set as the mean slope (0.024) of the Rio Behar catchment. Near-surface ice permeability is highly uncertain, but applying the $10^{-10} - 10^{-11}$ m^2 range estimated in Karlstrom et al. (2014), we estimate Darcy’s velocity v_d as $1.3 \times 10^{-4} - 10^{-5}$ m/s, one order smaller than the interfluvial

velocity v_h we quantified. This implies that interfluvial flow was not fully saturated in our study area, at least during the time when the ADCP supraglacial river discharge measurements were collected.

This is consistent with the idea that subsurface flow through permeable weathering crust ice is only partially saturated, except perhaps in regions near channel heads that exhibit many interconnected small lakes and fully saturated slush.

Partially-saturated subsurface flow can be described by the Boussinesq equation (Bear, 1972), obtained by combining Darcy's law for porous flow with continuity of water, forced by meltwater recharge due to melting (Karlstrom et al., 2014). The resultant partially-saturated (unconfined aquifer) velocity will be similar or lower than the fully-saturated velocity v_d – as shown in the Appendix III and Fig. 8, reasonable values result in $v_h \sim 10^{-4} - 10^{-5}$ m/s. Because neither of these simple models for porous flow matches the inferred meltwater velocity $v_h = 10^{-3} - 10^{-4}$ m/s in interfluvial zones of the Rio Behar catchment, we suspect that multiple physical processes are involved in v_h . For example, the combination of a relatively fast overland flow ($\sim 10^{-2}$ m/s) and a slower porous subsurface flow ($< 10^{-4}$ m/s), such as might occur for ephemeral channels on a variably saturated substrate, could explain the larger velocities. We leave mechanistic study of such issues to future work.

6.4 Advantages and Limitations of RWF and future directions

The Surface Routing and Lake Filling (SRLF) model is the first to attempt routing of surface meltwater downslope (Arnold et al., 1998). More recently, the Snyder Synthetic Unit Hydrograph (SUH) was used to derive moulin hydrographs (Smith et al., 2017). Both methods simulate observed moulin hydrographs reasonably well, but they cannot insightfully reveal the physical process of surface meltwater routing. Recently, permeable weathering crust was found on the Greenland bare-ice surface (Cooper et al., 2018), rather than impermeable bare ice as previously assumed (Arnold et al., 1998). For this reason, it may not be appropriate to apply principles of supraglacial open-channel flow everywhere on the ice surface, i.e. subsurface flows may be more suitable for describing meltwater transport in the interfluvial (hillslope) areas of higher-elevation ice separating meltwater channels. This reality calls for an easy-to-use, straightforward method to partition ice surface into channel vs. non-channel (i.e. interfluvial) flow with each experiencing different physical flow processes. The Rescaled Width Function (RWF) is our proposed solution for this partitioning.

We selected RWF over other SUH methods for the following reasons: 1) most SUH methods do not include interfluvial (hillslope) transport and consider only the open channel network on water routing (Singh et al., 2014), whereas RWF includes both hillslope and open-channel flows; 2) RWF is straightforward to implement and couple with remote sensing, requiring only hillslope and open-channel zones as inputs; 3) although RWF is a spatially-lumped model, it can provide catchment-scale meltwater routing velocities, which are crucial for broad-scale understanding of ice surface hydrology. The derived mean open-channel velocity is comparable to field-measured velocities in small supraglacial streams, and the derived hillslope velocity is comparable to simulations of a partially saturated subsurface hydrological model. Therefore, RWF appears to be a simple and useful tool for modeling meltwater routing across broad-scale areas of melting ice.

The central hypothesis of UH theory is that catchment response to rainfall (here, melt production) is linear, i.e., variations in input rainfall/melt change only the ordinates, not duration, of the direct hydrograph (Dingman, 2015). Meltwater routing is also assumed to be fully determinable by the morphometric characteristics of the catchment (here, IDCs drainage networks, shape, area, etc.) (Singh et al., 2014). These assumptions of linearity and fixed basin response simplify routing models but also create some limitations. Particularly, hydraulic geometries of meltwater channels are not independent of IDC characteristics but instead vary nonlinearly with channel discharge (i.e., $Q=wdv$, $w=aQ^b$, $d=cQ^f$, $v=kQ^m$). Gleason et al. (2016) suggest that supraglacial meltwater channels primarily accommodate greater discharges by increasing v_c ($m = 0.63 - 0.95$), which is also supported by Brykała (1999) ($m = 0.49$). Thus, at higher discharges open-channel flow velocities will increase nonlinearly. Moreover, v_h is also affected by surface melt dynamics (Leeson et al., 2012; Karlstrom et al., 2014; Karlstrom and Yang, 2016) and spatio-temporal patterns in surface meltwater production surely influence IDC hydrographic responses, just as spatio-temporal variations in rainfall pattern impact terrestrial hydrographic responses (Nicótina et al., 2008). Therefore, supraglacial IDCs may not respond to surface melt linearly. Future studies should consider varying v_h and v_c based on different surface melt patterns, which should generate variable RWFUHs during a melt season.

In addition to spatio-temporal variations in meltwater input, v_h and v_c surely vary spatially as well. RWF is a spatially-lumped hydrologic model yielding fixed constants of v_h and v_c averaged across the catchment (Table 1). However, in reality, v_h and v_c vary diversely within a catchment (Maidment et al., 1996; D'Odorico and Rigon, 2003). The SRLF model (Arnold et al., 1998) offers spatially varying surface meltwater routing velocities based on ice surface topography much like distributed terrestrial hydrologic models (Maidment et al., 1996; Liu et al., 2003), thus providing a physical based approach to investigate spatially-varying meltwater routing velocities. Therefore, combining RWF and SRLF would be a promising future direction for producing a physically based, spatially-distributed surface routing model for use on ice sheets. As a starting point, RWF-derived interfluvial travel velocities could be included in the SRLF model to parameterize meltwater flows through bare, porous low-density bare ice (Cooper et al., 2018), especially for partially saturated subsurface conditions. We leave spatially-distributed routing models for future studies because of two reasons: first, these models need more data inputs and parameters (which are difficult to estimate) than RWF; second, we need to determine what additional scientific value would be gained from more complex models.

Although the four RWF-based approaches presented here (non-conservative mapped rivers, conservative mapped rivers, high A_c threshold, low A_c threshold, see Fig. 6) all simulate the Rio Behar moulin hydrograph reasonably well, it is important to interpret each method from a physically-based standpoint and “get the right answers for the right reasons” (Kirchner, 2006). The four RWF-based approaches all perform well because we calibrated v_h and v_c from field and remote sensing observations and then used the optimal velocity combination to recreate a measured hydrograph. However, these bulk calibrated v_h and v_c values may or may not be reasonable estimates for channel and interfluvial velocities more broadly. They were collected using field and remote sensing observations collected during a narrow window of time, from 21-23 July 2015 when snow was gone and the Rio Behar IDC supraglacial stream/river network was highly developed on fully bare ice. We are encouraged that our derived values agree broadly with other field studies (McGrath et al., 2011; Chandler et al., 2013),

but additional field investigations are needed to confirm that the mean values of v_h and v_c derived here may be usefully applied to other bare-ice locations on the ice sheet.

6.5 Field site and observation recommendation

Selecting of an IDC for field study is logistically challenging and requires careful planning and design. We selected the Rio Behar catchment by considering surface melt intensity, distance to ice edge, distance to automatic weather stations, catchment size and shape, catchment outlet (moulin) conditions, and safety conditions (Smith et al., 2017). Two types of field measurements will be crucial for better understanding of surface meltwater routing process: supraglacial river discharge and subglacial water pressure. Supraglacial river discharge hydrographs can be used to validate the performance of surface meltwater routing methods, while subglacial water pressure can be used to estimate the hydrological responses of subglacial environments to different supraglacial meltwater inputs (moulin discharge).

In-situ investigation is also necessary to characterize interfluvial conditions. Cooper et al. (2018) analyzed the density and hydrological properties of bare, ablating ice away from open channels, by drilling holes into wet bare ice and measuring the subsurface porosity and water infilling rate, properties that cannot be measured from remote sensing. Satellite images are certainly useful for providing preliminary observations for ice surface conditions. For example, Smith et al. (2017) partitioned bare ice and snowpack zones using high-resolution satellite imagery and Ryan et al. (2018) investigated ice surface albedo, surface impurities, and cryoconite holes using higher-resolution UAV images. That said, we are unaware of any remote sensing solution to confirm presence/absence of saturated subsurface weathering crust and its hydraulic conductivity, so field measurements remain essential at present.

6.6 Future research directions

It is crucial to couple surface meltwater routing models with subglacial hydrological models to build a complete understanding of surface-to-bed meltwater connections. One path forward would be to use SUH, SRLF, and/or RWF to calculate moulin hydrographs using DEMs of different sources and spatial resolutions, then coupling this output to the Subglacial Hydrology and Kinetic, Transient Interactions (SHaKTI) subglacial hydrology model (Sommers et al., 2018). Doing so would allow derivation of hourly changes in subglacial water pressure in response to different moulin discharge inputs. A logical next step would be to then analyze the potential impact of these varying subglacial water pressures on subglacial hydrologic system evolution and ice flow dynamics. An ultimate objective should be to model the complete surface-to-bed meltwater transfer process by using RCMs to generate surface melt, surface routing to generate moulin discharge hydrographs, and subglacial models to track basal water pressure, subglacial hydrological system evolution, and ice flow.

Crucial ice surface topographic characteristics, such as slope, flow direction, flow length, drainage area, and drainage networks, are scale-dependent. Zhang and Montgomery (1994) illustrated DEM resolution significantly impacts hydrological

responses of terrestrial catchment to rainfall, using 2 m, 4 m, 10 m, 30 m, and 90 m DEMs. We suggest that DEM source and catchment geo-morphometry both affect a DEM's capability for simulating meltwater routing on the ice surface. In general, a 100 m or coarser resolution DEM may yield larger offsets in simulating moulin hydrographs compared to a 30 m resolution DEM but the specific offsets need further estimation. Moreover, high-resolution ArcticDEM (Noh and Howat, 2015, 2017) raises prospects for studying meltwater routing in unprecedented detail and it covers the entire Greenland Ice Sheet at present. The ArcticDEM products are now released at 2 m, 10 m, 32 m, 100 m, 500 m, and 1000 m resolution (Release 7, September 2018). Therefore, we recommend using ArcticDEM products in future meltwater routing studies.

A particularly promising area for future work will be incorporating surface routing delays in studies of proglacial discharge, in order to remove the effects of supraglacial delays before interpreting subglacial delays and/or storages from proglacial river discharge hydrographs. For example, in southwestern Greenland, numerous supraglacial IDCs form on the ice surface each summer and route meltwater into moulins (Thomsen et al., 1989; Banwell et al., 2012; Banwell et al., 2013; Arnold et al., 2014; Yang and Smith, 2016). By integrating RWF surface routing with the lumped supra-/en-/sub-glacial delays obtained from proglacial river studies (Rennermalm et al., 2013; Van As et al., 2014; Van As et al., 2017), subglacial runoff delays can be better separated from supraglacial delays. The corrected subglacial delays could then be used to better interpret the coupling of surface melt/runoff with subglacial water pressures (van de Wal et al., 2015; Wright et al., 2016), and used more generally to investigate the evolution of subglacial hydrological system over short time scales (Banwell et al., 2013; Andrews et al., 2014). As a simple example, the supraglacial delay we obtain here for Rio Behar catchment using RWF is ~0.5 days (11 hours), whereas the lumped delay obtained from Van As et al. (2017) is 3.9 days. This suggests subglacial delays contributed ~90% of the total delay between runoff generation on the ice sheet and its appearance in proglacial river discharge at the ice edge.

7. Conclusions

Numerous internally drained catchments (IDCs) are distributed on the southwest Greenland Ice Sheet. These catchments collect and drain meltwater through supraglacial stream/river networks to large, terminal outlet moulins, consequently constraining the timing and discharge of meltwater flowing over the ice surface to moulins that deliver meltwater to discrete locations on the bed. A growing literature is recognizing the non-trivial influence of supraglacial meltwater transport processes on meltwater received at the bed and proglacial zone. This study has investigated surface meltwater routing processes in Rio Behar catchment, a moderate-sized IDC near Kangerlussuaq, using high-resolution satellite and UAV observations and an in situ field-measured supraglacial river discharge hydrograph collected in late July 2015. Key meltwater routing parameters were quantified using a Rescaled Width Function (RWF) surface routing model which distinguishes fast meltwater transport through supraglacial stream/river channels from slow transport over interfluvies, the latter likely involving partially-saturated, near-surface porous-media flow. Our main contribution is thus to partition interfluvial vs. open-channel flow in a surface routing model adapted for use on ice surfaces, using remote sensing and sparse

in situ measurements. The model includes two terrestrial hydrologic techniques (unit hydrograph and rescaled width function) in a simple and flexible approach. Its scientific utility includes quantifying runoff delays on the Greenland ice sheet, improved understanding of open-channel versus interfluvial water transport on bare melting ice, improved interpretation of proglacial river discharge hydrographs, and improved coupling of climate/SMB datasets with subglacial borehole studies and models of subglacial hydrology and ice dynamics.

Acknowledgements

Kang Yang acknowledges support from the National Natural Science Foundation of China (41501452), the National Key R&D Program (2017YFB0504205), and the Fundamental Research Funds for the Central Universities. Laurence C. Smith and Matthew G. Cooper acknowledge the support of the NASA Cryosphere Program (NNX14AH93G) managed by Dr. Thomas Wagner. Leif Karlstrom acknowledges support from the NASA Rapid Response and Novel Research in Earth Science (NNX16AQ56G). Dirk van As acknowledges the support of the Greenland Analogue Project (GAP) and the Programme for Monitoring of the Greenland Ice Sheet (PROMICE). WorldView imagery and geospatial support for this work were provided by the Polar Geospatial Center, University of Minnesota, under NSF PLR awards 1043681 & 1559691. We thank Michael Willis for providing high-resolution WorldView DEMs.

Appendix I: Parameter settings in the SRLF model

In the SRLF model, for each bare ice pixel, meltwater flow velocity (v) is calculated using Manning's equation:

$$v = R^{2/3} S^{1/2} / n \quad (1)$$

where R is the hydraulic radius of the meltwater channel, S is ~~water-ice~~ surface slope calculated from DEM, and n is the Manning roughness coefficient. We used the mean ice surface slope as an approximate for the channel slope because we do not have any in situ small channel slope measurements.

Most supraglacial streams flow in a series of small and sub-parallel channels and thereby Arnold et al. (1998) used a small, constant value of $R = 0.035$ m for all pixels; in this case, if stream width/depth ratio is set to 5.0 (Karlstrom et al., 2014) (4.5 reported in Yang et al. (2016) and 3.4-12.0 in Knighton (1981)) and a rectangle channel cross section is assumed, stream depth is calculated as ~0.049 m, which is very close to field-measured 0.050 m (Karlstrom et al., 2014) and within the range of 0.030-0.400 m reported in Gleason et al. (2016). Moreover, Arnold et al. (1998) assumed Manning's n as 0.05, which is also supported by field measurements (e.g., $n = 0.035 \pm 0.027$ reported in Gleason et al. (2016), and 0.007 – 0.063 reported in Brykala (1999)). This value is notably larger than the value used in Leeson et al. (2012), i.e., $n = 0.011$, which was derived experimentally for ice by Lotter (1933). We suggest that field-measured n values of supraglacial channels are more accurate than experimental estimation because some plausible mechanisms (e.g., longitudinal cracks that “intersect

channels and persist in the bed” (Gleason et al., 2016), cryoconite pitting, and variable ice bed forms) can increase bed roughness and thereby yield high n values.

Appendix II: Width function

Width Function (WF) is a widely used hydrologic modeling method in terrestrial catchment studies and provides an easy-to-use, spatially-lumped approach to quantify the influence of the river network geomorphology on the hydrologic response of a catchment (D’Odorico and Rigon, 2003). The WF of a catchment is computed as the number of pixels located at a given distance from the outlet following the river network (L_c), normalized by the total number of pixels belonging to the river network (Singh et al., 2014). If a constant water flow velocity (v_c) is assumed, travel time t can be calculated for all the channel pixels, i.e., $t = L_c/v_c$, and consequently catchment UH can be derived, which was named as WFUH (Singh et al., 2014). The WFUH performs well for large terrestrial catchments in which the travel time across the interfluvial zone is negligible with respect to that in the river network (D’Odorico and Rigon, 2003). However, on the ice surface, interfluvial processes are important (or even dominate) (Arnold et al., 1998; Karlstrom et al., 2014) and thereby should not be excluded.

Appendix III: Boussinesq approximation to porous flow

Velocity of unchanneled subsurface flow may be estimated through the Boussinesq approximation to porous flow in an unconfined aquifer (geometry defined in Fig. 8), for which Darcy’s Law combined with continuity yields a second order ordinary differential equation (Bear, 1972) that may be solved to find the steady state solution for subsurface water height h as a function of distance x away from a stream:

$$h(x) = \left[h_0^2 - \frac{x}{L} (h_0^2 - h_L^2) + \frac{M}{k} (L - x)x \right]^{1/2} \quad (2)$$

where M is the rate of melting (m/s) derived from surface energy budget, h_0 and h_L are stream depths on either side of the porous unchanneled zone, and $k = \kappa \rho g / \mu$ is the hydraulic conductivity of the porous ice with κ the permeability, ρ ice density, g gravity and μ the dynamics viscosity of water.

The water divide, where $h(x)$ reaches a maximum, is given by

$$x_w = \frac{L}{2} - \frac{k}{M} \frac{(h_0^2 - h_L^2)}{2L}. \quad (3)$$

For simplicity we will study the case where $h_0 = h_L$ so $x_w = \frac{L}{2}$. The velocity of flow v_h at any point x is given by $v_h = k dh/dx$, and the average velocity magnitude on either side of the water divide is

$$v_h = \alpha \left[\sqrt{1 + \frac{kM}{\alpha^2}} - 1 \right] \quad (4)$$

where $\alpha = 2kh_0/L$. If $\frac{kM}{\alpha^2} \gg 1$, as we will find in this case, the velocity is well approximated by

$$v_h \sim \sqrt{kM} - \alpha . \quad (5)$$

Although few direct measurements of α exist, we estimate based on field-determined permeabilities of Karlstrom et al. (2014) that $k \sim 10^{-4} - 10^{-3}$ m/s, $h_0 \sim 0.1 - 1$ m, $L \sim 1 - 100$ m, and $M \sim 10^{-5} - 10^{-4}$ m/s. This range implies $\frac{kM}{\alpha^2} \gg 1$, and subsequently $v_h \sim 10^{-5} - 10^{-4}$ m/s.

5 Appendix IV: Meltwater channel width distribution of supraglacial stream/river network

The meltwater channel width was derived using ArcScan tool of the ArcGIS software and width histogram of conservatively mapped supraglacial stream/river networks is shown in Fig. 9. This distribution shows that most supraglacial meltwater channels are narrower than 4 m and the resultant mean channel width is 2.5 ± 2.0 m, supporting our conclusion that numerous small supraglacial streams control bulk-catchment channel velocity v_c . We defined large supraglacial rivers as the features that can be identified by moderate-resolution (10 – 30 m) satellites (e.g., Sentinel-2 and Landsat-8), while small supraglacial streams as the features that can only be identified by high-resolution (0.5 – 2.0 m) satellites (e.g., WorldView-1/2/3/4). It is subjective to determine a threshold width but if required, we recommend 10 m.

References

- Andrews, L. C., Catania, G. A., Hoffman, M. J., Gulley, J. D., Luthi, M. P., Ryser, C., Hawley, R. L., and Neumann, T. A.: Direct observations of evolving subglacial drainage beneath the Greenland Ice Sheet, *Nature*, 514, 80-83, <https://doi.org/10.1038/nature13796>, 2014.
- 5 Arnold, N. S., Richards, K., Willis, I., and Sharp, M.: Initial results from a distributed, physically based model of glacier hydrology, *Hydrolo. Process.*, 12, 191-219, [https://doi.org/10.1002/\(SICI\)1099-1085\(199802\)12:2<191::AID-HYP571>3.0.CO;2-C](https://doi.org/10.1002/(SICI)1099-1085(199802)12:2<191::AID-HYP571>3.0.CO;2-C), 1998.
- Arnold, N. S., Banwell, A. F., and Willis, I. C.: High-resolution modelling of the seasonal evolution of surface water storage on the Greenland Ice Sheet, *Cryosph.*, 8, 1149-1160, <https://doi.org/10.5194/tc-8-1149-2014>, 2014.
- Banwell, A. F., Arnold, N. S., Willis, I. C., Tedesco, M., and Ahlström, A. P.: Modeling supraglacial water routing and lake filling on the
10 Greenland Ice Sheet, *J. Geophys. Res.*, 117, F04012, <https://doi.org/10.1029/2012jf002393>, 2012.
- Banwell, A. F., Willis, I. C., and Arnold, N. S.: Modeling subglacial water routing at Paakitsoq, W Greenland, *J. Geophys. Res. Earth Surf.*, 118, 1282-1295, <https://doi.org/10.1002/jgrf.20093>, 2013.
- Banwell, A. F., Hewitt, I., Willis, I., and Arnold, N.: Moulin density controls drainage development beneath the Greenland Ice Sheet, *J. Geophys. Res. Earth Surf.*, 121, 2248-2269, <https://doi.org/10.1002/2015JF003801>, 2016.
- 15 Bear, J.: *Dynamics of Fluids in Porous Media*, Dover Publications, New York, 1972.
- Brykala, D.: Hydraulic geometry of a supraglacial stream on the Waldemar Glacier (Spitsbergen) in the summer of 1997, *Polish Polar Studies : 26th International Polar Symposium*, Lublin, Poland, 1999, 51-64,
- Chandler, D. M., Wadham, J. L., Lis, G. P., Cowton, T., Sole, A., Bartholomew, I., Telling, J., Nienow, P., Bagshaw, E. B., Mair, D., Vinen, S., and Hubbard, A.: Evolution of the subglacial drainage system beneath the Greenland Ice Sheet revealed by tracers, *Nat. Geosci.*, 6, 195-198, <https://doi.org/10.1038/ngeo1737>, 2013.
- 20 Clason, C. C., Mair, D. W. F., Nienow, P. W., Bartholomew, I. D., Sole, A., Palmer, S., and Schwanghart, W.: Modelling the transfer of supraglacial meltwater to the bed of Leverett Glacier, Southwest Greenland, *Cryosph.*, 9, 123-138, <https://doi.org/10.5194/tc-9-123-2015>, 2015.
- Collins, W. T.: Runoff distribution graphs from precipitation occurring in more than one time unit, *Civil Eng.*, 9, 559-561, 1939.
- 25 Cooper, M. G., Smith, L. C., Rennermalm, A. K., Miège, C., Pitcher, L. H., Ryan, J. C., Yang, K., and Cooley, S.: Meltwater storage in low-density near-surface bare ice in the Greenland ice sheet ablation zone, *Cryosph.*, 12, 955-970, <https://doi.org/10.5194/tc-2017-107>, 2018.
- Crozier, J., Karlstrom, L., and Yang, K.: Basal control of supraglacial meltwater catchments on the Greenland Ice Sheet, *Cryosph.*, 12, 3383-3407, <https://doi.org/10.5194/tc-12-3383-2018>, 2018.
- 30 Cullather, R. I., Nowicki, S. M. J., Zhao, B., and Koenig, L. S.: A Characterization of Greenland Ice Sheet Surface Melt and Runoff in Contemporary Reanalyses and a Regional Climate Model, *Front. Earth Sci.*, 4, <https://doi.org/10.3389/feart.2016.00010>, 2016.
- D'Odorico, P., and Rigon, R.: Hillslope and channel contributions to the hydrologic response, *Water Resour. Res.*, 39, 1113, <https://doi.org/10.1029/2002WR001708>, 2003.

- de Fleurian, B., Morlighem, M., Seroussi, H., Rignot, E., van den Broeke, M. R., Kuipers Munneke, P., Mouginot, J., Smeets, P. C. J. P., and Tedstone, A. J.: A modeling study of the effect of runoff variability on the effective pressure beneath Russell Glacier, West Greenland, *J. Geophys. Res. Earth Surf.*, 121, 1834-1848, <https://doi.org/10.1002/2016JF003842>, 2016.
- Di Lazzaro, M.: Regional analysis of storm hydrographs in the Rescaled Width Function framework, *J. Glaciol.*, 373, 352-365, <http://doi.org/10.1016/j.jhydrol.2009.04.027>, 2009.
- Dingman, S. L.: Physical hydrology (3rd edition), Waveland press, 2015.
- Elliston, G. R.: Water movement through the Gornergletscher, *International Association of Scientific Hydrology*, 95, 79-84, 1973.
- Fettweis, X., Franco, B., Tedesco, M., van Angelen, J. H., Lenaerts, J. T. M., van den Broeke, M. R., and Gallée, H.: Estimating the Greenland ice sheet surface mass balance contribution to future sea level rise using the regional atmospheric climate model MAR, *Cryosph.*, 7, 469-489, <https://doi.org/10.5194/tc-7-469-2013>, 2013.
- Fitzpatrick, A. A. W., Hubbard, A. L., Box, J. E., Quincey, D. J., van As, D., Mikkelsen, A. P. B., Doyle, S. H., Dow, C. F., Hasholt, B., and Jones, G. A.: A decade of supraglacial lake volume estimates across a land-terminating margin of the Greenland Ice Sheet, *Cryosph.*, 8, 107-121, <https://doi.org/10.5194/tc-8-107-2014>, 2014.
- Fountain, A. G., and Walder, J. S.: Water flow through temperate glaciers, *Rev. Geophys.*, 36, 299-328, <https://doi.org/10.1029/97RG03579>, 1998.
- Gleason, C. J., Smith, L. C., Chu, V. W., Legleiter, C. J., Pitcher, L. H., Overstreet, B. T., Rennermalm, A. K., Forster, R. R., and Yang, K.: Characterizing supraglacial meltwater channel hydraulics on the Greenland Ice Sheet from in situ observations, *Earth Surf. Process. Landf.*, 41, 2111-2122, <https://doi.org/10.1002/esp.3977>, 2016.
- Howat, I. M., Negrete, A., and Smith, B. E.: The Greenland Ice Mapping Project (GIMP) land classification and surface elevation data sets, *Cryosph.*, 8, 1509-1518, <https://doi.org/10.5194/tc-8-1509-2014>, 2014.
- Ignéczi, Á., Sole, A. J., Livingstone, S. J., Ng, F. S. L., and Yang, K.: Greenland Ice Sheet surface topography and drainage structure controlled by the transfer of basal variability, *Front. Earth Sci.*, 6, 101, 2018.
- Irvine-Fynn, T. D. L., Hodson, A. J., Moorman, B. J., Vatne, G., and Hubbard, A. L.: Polythermal glacier hydrology: a review, *Rev. Geophys.*, 49, RG4002, <https://doi.org/10.1029/2010RG000350>, 2011.
- Karlstrom, L., Zok, A., and Manga, M.: Near-surface permeability in a supraglacial drainage basin on the Llewellyn Glacier, Juneau Icefield, British Columbia, *Cryosph.*, 8, 537-546, <https://doi.org/10.5194/tc-8-537-2014>, 2014.
- Karlstrom, L., and Yang, K.: Fluvial supraglacial landscape evolution on the Greenland Ice Sheet, *Geophys. Res. Lett.*, 43, 2683-2692, <https://doi.org/10.1002/2016GL067697>, 2016.
- Kesseli, J. E.: The Concept of the Graded River, *J. Geol.*, 49, 561-588, 1941.
- King, L., Hassan, M., Yang, K., and Flowers, G.: Flow routing for delineating supraglacial meltwater channel networks, *Remote Sens.*, 8, 988, <https://doi.org/10.3390/rs8120988>, 2016.
- Kirchner, J. W.: Getting the right answers for the right reasons: Linking measurements, analyses, and models to advance the science of hydrology, *Water Resour. Res.*, 42, W03S04, <https://doi.org/10.1029/2005WR004362>, 2006.
- Knighton, A. D.: Channel form and flow characteristics of supraglacial streams, Austre Okstindbreen, Norway, *Arct. Antarct. Alp. Res.*, 13, 295-306, 1981.
- Lampkin, D. J., and VanderBerg, J.: A preliminary investigation of the influence of basal and surface topography on supraglacial lake distribution near Jakobshavn Isbrae, western Greenland, *Hydrolo. Process.*, 25, 3347-3355, 10.1002/hyp.8170, 2011.

- Lampkin, D. J., and VanderBerg, J.: Supraglacial melt channel networks in the Jakobshavn Isbræ region during the 2007 melt season, *Hydrolo. Process.*, 28, 6038-6053, <https://doi.org/10.1002/hyp.10085>, 2014.
- Leeson, A. A., Shepherd, A., Palmer, S., Sundal, A., and Fettweis, X.: Simulating the growth of supraglacial lakes at the western margin of the Greenland ice sheet, *Cryosph.*, 6, 1077-1086, <https://doi.org/10.5194/tc-6-1077-2012>, 2012.
- 5 Lefebvre, F., Gallée, H., van Ypersele, J.-P., and Greuell, W.: Modeling of snow and ice melt at ETH Camp (West Greenland): A study of surface albedo, *J. Geophys. Res. Atmospheres*, 108, 16, <https://doi.org/10.1029/2001JD001160>, 2003.
- Lindsay, J. B.: The practice of DEM stream burning revisited, *Earth Surf. Process. Landf.*, 41, 658-668, <https://doi.org/10.1002/esp.3888>, 2016.
- Liu, Y. B., Gebremeskel, S., De Smedt, F., Hoffmann, L., and Pfister, L.: A diffusive transport approach for flow routing in GIS-based flood modeling, *J. Hydrol.*, 283, 91-106, [https://doi.org/10.1016/S0022-1694\(03\)00242-7](https://doi.org/10.1016/S0022-1694(03)00242-7), 2003.
- 10 Lotter, G. K.: Considerations on hydraulic design of channels with different roughness of walls, *Transactions of All-Union Scientific Research Institute of Hydraulic Engineering*, 9, 238-241, 1933.
- Mackin, J. H.: Concept of the graded river, *GSA Bulletin*, 59, 463-512, [https://doi.org/10.1130/0016-7606\(1948\)59\[463:COTGR\]2.0.CO;2](https://doi.org/10.1130/0016-7606(1948)59[463:COTGR]2.0.CO;2), 1948.
- 15 Maidment, D. R., Olivera, F., Calver, A., Eatherall, A., and Fraczek, W.: Unit hydrograph derived from a spatially distributed velocity field, *Hydrolo. Process.*, 10, 831-844, [https://doi.org/10.1002/\(SICI\)1099-1085\(199606\)10:6<831::AID-HYP374>3.0.CO;2-N](https://doi.org/10.1002/(SICI)1099-1085(199606)10:6<831::AID-HYP374>3.0.CO;2-N), 1996.
- Mays, L. W.: *Water Resources Engineering*, 2nd ed., Wiley, 928 pp., 2010.
- McGrath, D., Colgan, W., Steffen, K., Lauffenburger, P., and Balog, J.: Assessing the summer water budget of a moulin basin in the Sermeq Avannarleq ablation region, Greenland ice sheet, *J. Glaciol.*, 57, 954-964, <https://doi.org/10.3189/002214311798043735>, 2011.
- 20 Montgomery, D. R., and Dietrich, W. E.: Source areas, drainage density, and channel initiation, *Water Resour. Res.*, 25, 1907-1918, <https://doi.org/10.1029/WR025i008p01907>, 1989.
- Montgomery, D. R., and Dietrich, W. E.: Channel initiation and the problem of landscape scale, *Science*, 255, 826, <https://doi.org/10.1126/science.255.5046.826>, 1992.
- 25 Montgomery, D. R., and Foufoula-Georgiou, E.: Channel network source representation using digital elevation models, *Water Resour. Res.*, 29, 3925-3934, <https://doi.org/10.1029/93WR02463>, 1993.
- Moussa, R.: What controls the width function shape, and can it be used for channel network comparison and regionalization?, *Water Resour. Res.*, 44, W08456, <https://doi.org/10.1029/2007WR006118>, 2008.
- Müller, F., and Keeler, C. M.: Errors in short-term ablation measurements on melting ice surfaces, *J. Glaciol.*, 8, 91-105, <https://doi.org/10.3189/S0022143000020785>, 1969.
- 30 Mutzner, R., Tarolli, P., Sofia, G., Parlange, M. B., and Rinaldo, A.: Field study on drainage densities and rescaled width functions in a high-altitude alpine catchment, *Hydrolo. Process.*, 30, 2138-2152, <https://doi.org/10.1002/hyp.10783>, 2016.
- Nash, J. E., and Sutcliffe, J. V.: River flow forecasting through conceptual models part I — A discussion of principles, *J. Hydrol.*, 10, 282-290, [https://doi.org/10.1016/0022-1694\(70\)90255-6](https://doi.org/10.1016/0022-1694(70)90255-6), 1970.
- 35 Nicótina, L., Alessi Celegon, E., Rinaldo, A., and Marani, M.: On the impact of rainfall patterns on the hydrologic response, *Water Resour. Res.*, 44, W12401, <https://doi.org/10.1029/2007WR006654>, 2008.

- Noh, M.-J., and Howat, I. M.: Automated stereo-photogrammetric DEM generation at high latitudes: Surface Extraction with TIN-based Search-space Minimization (SETSM) validation and demonstration over glaciated regions, *GISci. Remote Sens.*, 52, 198-217, <https://doi.org/10.1080/15481603.2015.1008621>, 2015.
- Noh, M.-J., and Howat, I. M.: The Surface Extraction from TIN based Search-space Minimization (SETSM) algorithm, *ISPRS J. Photogramm. Remote Sens.*, 129, 55-76, <https://doi.org/10.1016/j.isprsjprs.2017.04.019>, 2017.
- Poinar, K., Joughin, I., Das, S. B., Behn, M. D., Lenaerts, J. T. M., and van den Broeke, M. R.: Limits to future expansion of surface-melt-enhanced ice flow into the interior of western Greenland, *Geophys. Res. Lett.*, 42, 1800-1807, <https://doi.org/10.1002/2015GL063192>, 2015.
- Rennermalm, A. K., Smith, L. C., Chu, V. W., Box, J. E., Forster, R. R., Van den Broeke, M. R., Van As, D., and Moustafa, S. E.: Evidence of meltwater retention within the Greenland ice sheet, *Cryosph.*, 7, 1433-1445, <https://doi.org/10.5194/tc-7-1433-2013>, 2013.
- Ryan, J. C., Hubbard, A. L., Box, J. E., Todd, J., Christoffersen, P., Carr, J. R., Holt, T. O., and Snooke, N.: UAV photogrammetry and structure from motion to assess calving dynamics at Store Glacier, a large outlet draining the Greenland ice sheet, *Cryosph.*, 9, 1-11, <https://doi.org/10.5194/tc-9-1-2015>, 2015.
- Ryan, J. C., Hubbard, A., Stibal, M., Irvine-Fynn, T. D., Cook, J., Smith, L. C., Cameron, K., and Box, J.: Dark zone of the Greenland Ice Sheet controlled by distributed biologically-active impurities, *Nat. Commun.*, 9, 1065, <https://doi.org/10.1038/s41467-018-03353-2>, 2018.
- Shean, D. E., Alexandrov, O., Moratto, Z. M., Smith, B. E., Joughin, I. R., Porter, C., and Morin, P.: An automated, open-source pipeline for mass production of digital elevation models (DEMs) from very-high-resolution commercial stereo satellite imagery, *ISPRS J. Photogramm. Remote Sens.*, 116, 101-117, <https://doi.org/10.1016/j.isprsjprs.2016.03.012>, 2016.
- Singh, P. K., Mishra, S. K., and Jain, M. K.: A review of the synthetic unit hydrograph: from the empirical UH to advanced geomorphological methods, *Hydrolog. Sci. J.*, 59, 239-261, <https://doi.org/10.1080/02626667.2013.870664>, 2014.
- Smith, L. C., Chu, V. W., Yang, K., Gleason, C. J., Pitcher, L. H., Rennermalm, A. K., Legleiter, C. J., Behar, A. E., Overstreet, B. T., Moustafa, S. E., Tedesco, M., Forster, R. R., LeWinter, A. L., Finnegan, D. C., Sheng, Y., and Balog, J.: Efficient meltwater drainage through supraglacial streams and rivers on the southwest Greenland ice sheet, *Proc. Natl. Acad. Sci.*, 112, 1001-1006, <https://doi.org/10.1073/pnas.1413024112>, 2015.
- Smith, L. C., Yang, K., Pitcher, L. H., B.T., O., Chu, V. W., Rennermalm, A. K., Ryan, J., Cooper, M. G., Gleason, C. J., and Tedesco, M.: Direct measurements of meltwater runoff on the Greenland ice sheet surface, *Proc. Natl. Acad. Sci.*, 114, E10622-E10631, <https://doi.org/10.1073/pnas.1707743114>, 2017.
- Sole, A. J., Mair, D. W. F., Nienow, P. W., Bartholomew, I. D., King, M. A., Burke, M. J., and Joughin, I.: Seasonal speedup of a Greenland marine - terminating outlet glacier forced by surface melt-induced changes in subglacial hydrology, *J. Geophys. Res. Earth Surf.*, 116, <https://doi.org/10.1029/2010JF001948>, 2011.
- Sommers, A., Rajaram, H., and Morlighem, M.: SHAKTI: Subglacial Hydrology and Kinetic, Transient Interactions v1.0, *Geosci. Model Dev.*, 11, 2955-2974, <https://doi.org/10.5194/gmd-11-2955-2018>, 2018.
- Stevens, I. T., Irvine - Fynn, T. D. L., Porter, P. R., Cook, J. M., Edwards, A., Smart, M., Moorman, B. J., Hodson, A. J., and Mitchell, A. C.: Near - surface hydraulic conductivity of northern hemisphere glaciers, *Hydrolo. Process.*, 32, 850-865, <https://doi.org/10.1002/hyp.11439>, 2018.

- Thomsen, H. H., Thorning, L., and Olesen, O. B.: Applied glacier research for planning hydro-electric power, Ilulissat/Jakobshavn, West Greenland, *Ann. Glaciol.*, 13, 257-261, <https://doi.org/10.3189/S0260305500008004>, 1989.
- Van As, D., Andersen, M. L., Petersen, D., Fettweis, X., Van Angelen, J. H., Lenaerts, J. T. M., Van Den Broeke, M. R., Lea, J. M., Bøggild, C. E., Ahlstrøm, A. P., and Steffen, K.: Increasing meltwater discharge from the Nuuk region of the Greenland ice sheet and implications for mass balance (1960–2012), *J. Glaciol.*, 60, 314-322, <https://doi.org/10.3189/2014JoG13J065>, 2014.
- Van As, D., Bech Mikkelsen, A., Holtegaard Nielsen, M., Box, J., Claesson Liljedahl, L., Lindbäck, K., Pitcher, L., and Hasholt, B.: Hypsometric amplification and routing moderation of Greenland ice sheet meltwater release, *Cryosph.*, 11, 1371-1386, <https://doi.org/10.5194/tc-2016-285>, 2017.
- van de Wal, R. S. W., Smeets, C. J. P. P., Boot, W., Stoffelen, M., van Kampen, R., Doyle, S. H., Wilhelms, F., van den Broeke, M. R., Reijmer, C. H., Oerlemans, J., and Hubbard, A.: Self-regulation of ice flow varies across the ablation area in south-west Greenland, *Cryosph.*, 9, 603-611, <https://doi.org/10.5194/tc-9-603-2015>, 2015.
- Willis, I. C., Arnold, N. S., and Brock, B. W.: Effect of snowpack removal on energy balance, melt and runoff in a small supraglacial catchment, *Hydrolo. Process.*, 16, 2721-2749, <https://doi.org/10.1002/hyp.1067>, 2002.
- Wright, P. J., Harper, J. T., Humphrey, N. F., and Meierbachtol, T. W.: Measured basal water pressure variability of the western Greenland Ice Sheet: Implications for hydraulic potential, *J. Geophys. Res. Earth Surf.*, 121, 1134-1147, <https://doi.org/10.1002/2016JF003819>, 2016.
- Yang, K., Li, M., Liu, Y., Cheng, L., Huang, Q., and Chen, Y.: River detection in remotely sensed imagery using Gabor filtering and path opening, *Remote Sens.*, 7, 8779-8802, <https://doi.org/10.3390/rs70708779>, 2015a.
- Yang, K., Smith, L. C., Chu, V. W., Gleason, C. J., and Li, M.: A Caution on the Use of Surface Digital Elevation Models to Simulate Supraglacial Hydrology of the Greenland Ice Sheet, *IEEE J. Sel. Topics Appl. Earth Observ. Remote Sens.*, 8, 5212-5224, <https://doi.org/10.1109/JSTARS.2015.2483483>, 2015b.
- Yang, K., and Smith, L. C.: Internally drained catchments dominate supraglacial hydrology of the southwest Greenland Ice Sheet, *J. Geophys. Res. Earth Surf.*, 121, 1891-1910, <https://doi.org/10.1002/2016JF003927>, 2016.
- Yang, K., Smith, L. C., Chu, V. W., Pitcher, L. H., Gleason, C. J., Rennermalm, A. K., and Li, M.: Fluvial morphometry of supraglacial river networks on the southwest Greenland Ice Sheet, *GISci. Remote Sens.*, 53, 459-482, <https://doi.org/10.1080/15481603.2016.1162345>, 2016.
- Yang, K., Karlstrom, L., Smith, L. C., and Li, M.: Automated high resolution satellite image registration using supraglacial rivers on the Greenland Ice Sheet, *IEEE J. Sel. Topics Appl. Earth Observ. Remote Sens.*, 10, 845-856, <https://doi.org/10.1109/JSTARS.2016.2617822>, 2017.
- Zhang, W., and Montgomery, D. R.: Digital elevation model grid size, landscape representation, and hydrologic simulations, *Water Resour. Res.*, 30, 1019-1028, <https://doi.org/10.1029/93WR03553>, 1994.
- Zuo, Z., and Oerlemans, J.: Modelling albedo and specific balance of the Greenland ice sheet: calculations for the Søndre Strømfjord transect, *J. Glaciol.*, 42, 305-317, <https://doi.org/10.1017/S0022143000004160>, 1996.
- Zwally, H. J., Abdalati, W., Herring, T., Larson, K., Saba, J., and Steffen, K.: Surface melt-induced acceleration of Greenland ice-sheet flow, *Science*, 297, 218-222, <https://doi.org/10.1126/science.1072708>, 2002.

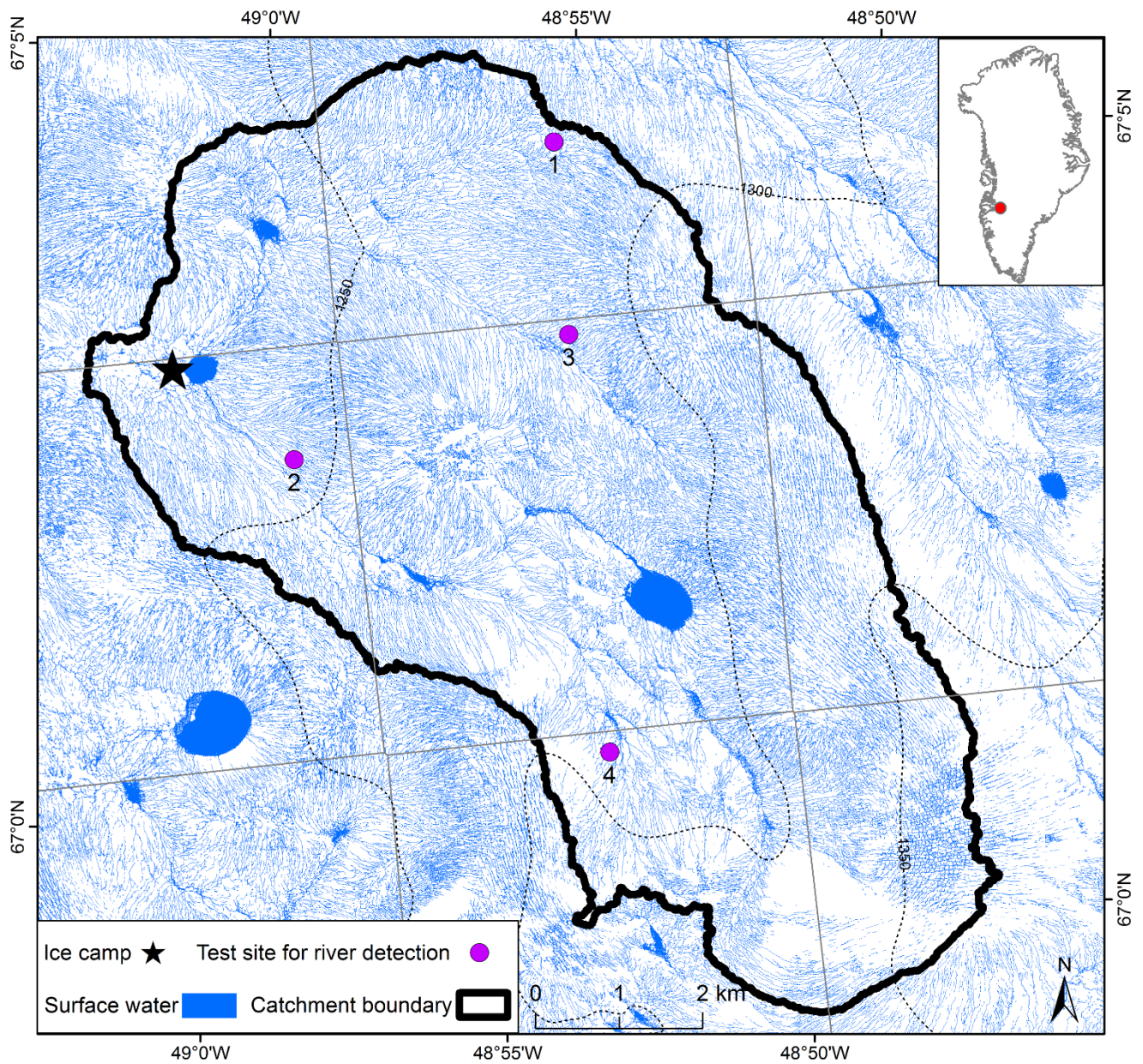


Figure 1. Rio Behar catchment is a moderate-sized internally drained catchment (IDC) on the southwest Greenland Ice Sheet. A highly developed supraglacial stream/river network was mapped from a high-resolution (0.5 m) panchromatic WorldView-1 (WV1) image acquired on 18 July 2015. The catchment outlet moulin is under the black star and 5 m MAR grid cells are shown in grey rectangles. A derivative 3 m resolution DEM is used to delineate the topographic catchment boundary (black line). An in situ hourly hydrograph of supraglacial river discharge collected by Smith et al. (2017) (black star) was used to calibrate a Rio Behar catchment Unit Hydrograph (UH) for the Rescaled Width Function (RWF) and Surface routing and lake filling (SRLF) surface routing models.

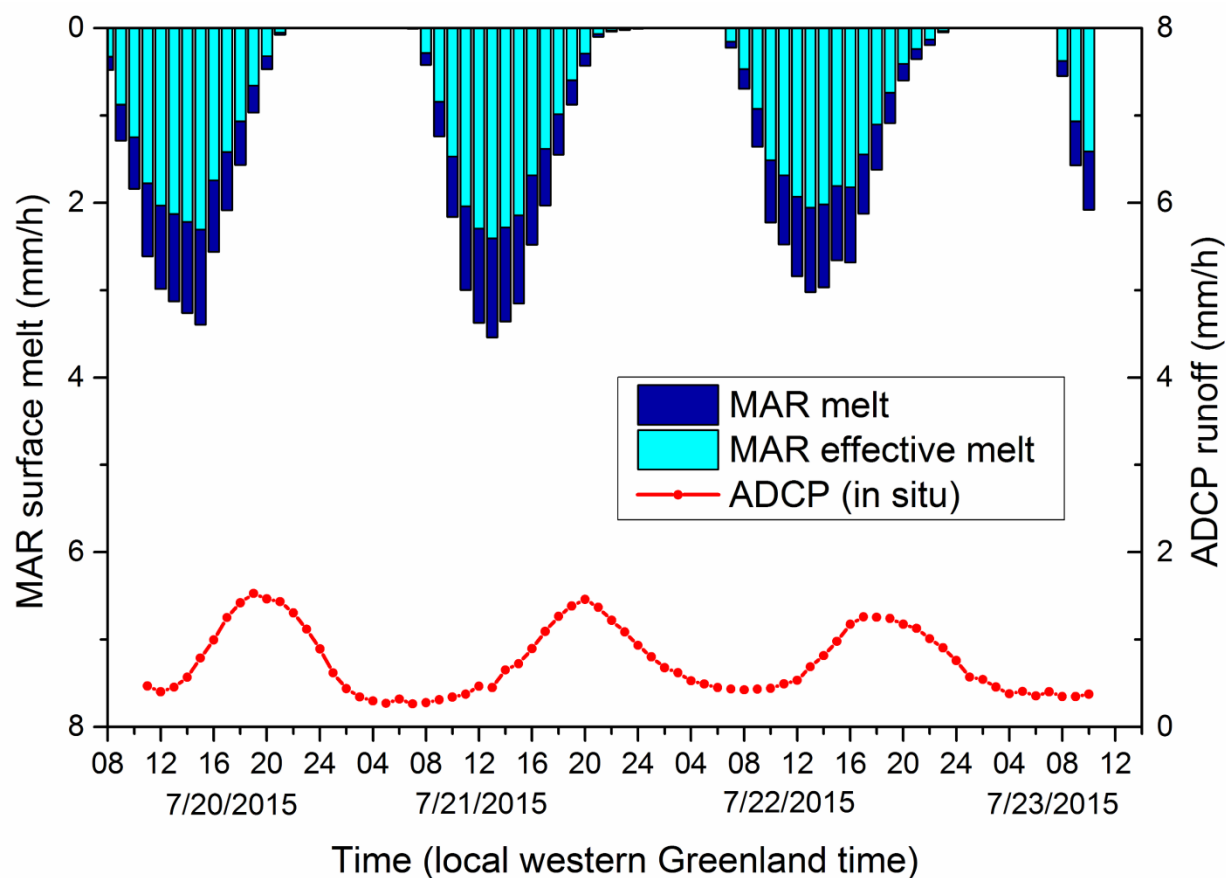


Figure 2. Within the Rio Behar catchment, MAR regional climate model inputs of melt (at top) are paired with in situ Acoustic Doppler Current Profiler (ADCP) outputs of supraglacial river discharge (at bottom) to calibrate the Unit Hydrograph (UH) surface routing models assessed in this study. “Effective melt” is the fraction of total MAR melt production that is transported all to the Rio Behar IDC terminal outlet moulin (Smith et al., 2017). The UH is calculated using effective melt as inputs and observed runoff as outputs as per (Smith et al., 2017).

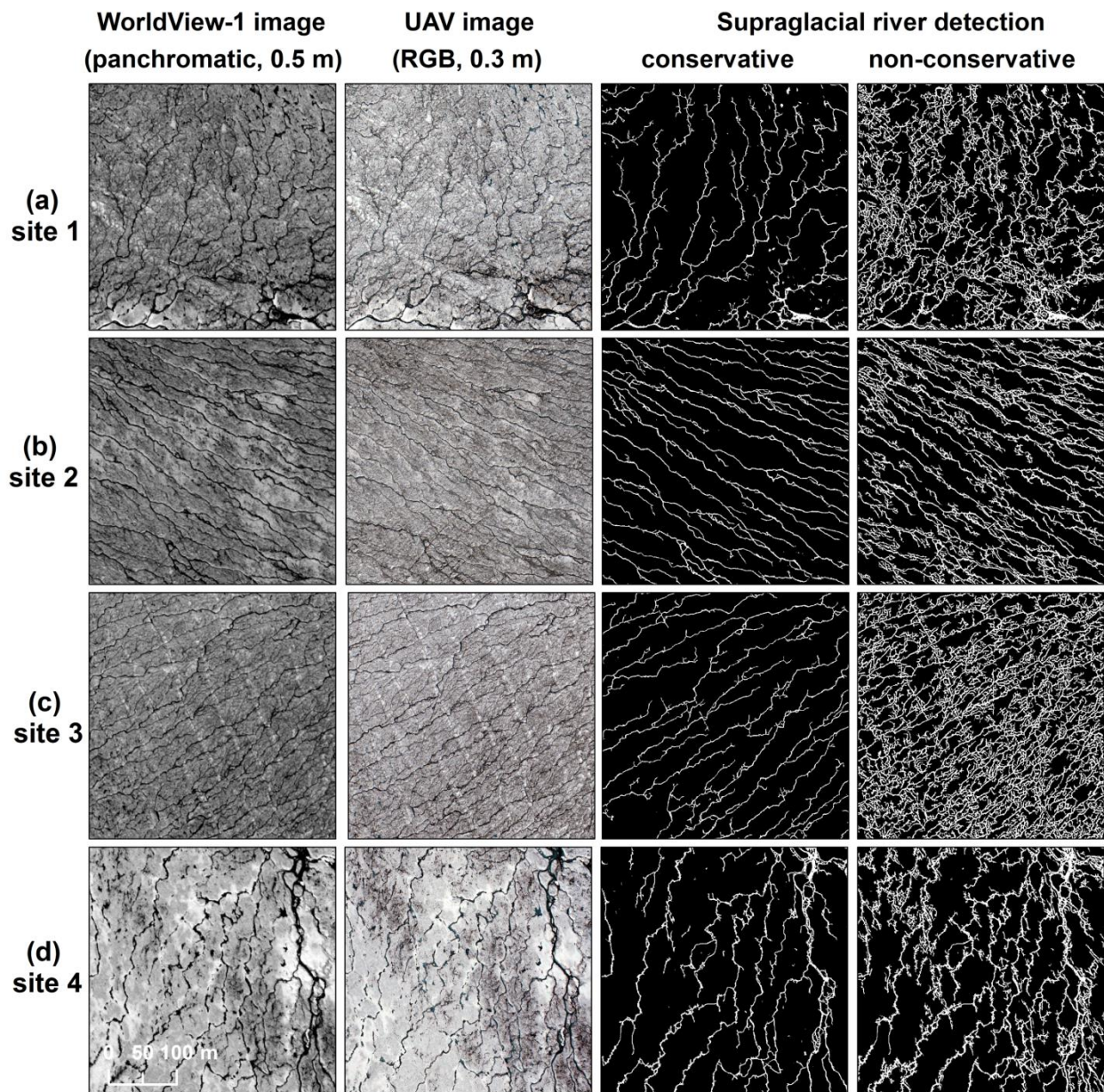


Figure 3. An 18 July 2015 panchromatic WorldView-1 (WV1) image (spatial resolution 0.5 m, column 1), concurrent UAV imagery (spatial resolution 0.3 m, column 2), and corresponding supraglacial rivers and streams delineated from the WV1 imagery for sites 1-4. Column 3 shows conservative detection of actively flowing channels, while column 4 shows non-conservative detection.

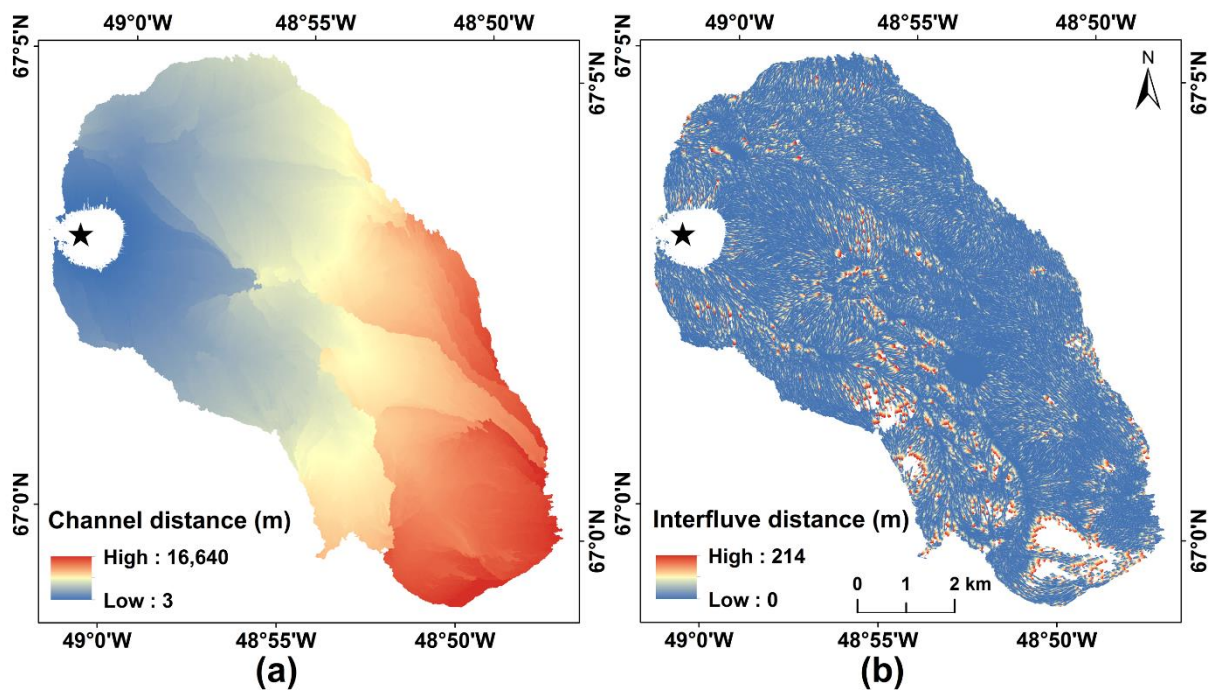


Figure 4. Meltwater travel distances for (a) open-channels; and (b) interfluves of the Rio Behar internally drained catchment (IDC) as obtained by “burning” the 18 July 2015 WorldView DEM with the conservative remotely sensed active supraglacial stream/river surface drainage network.

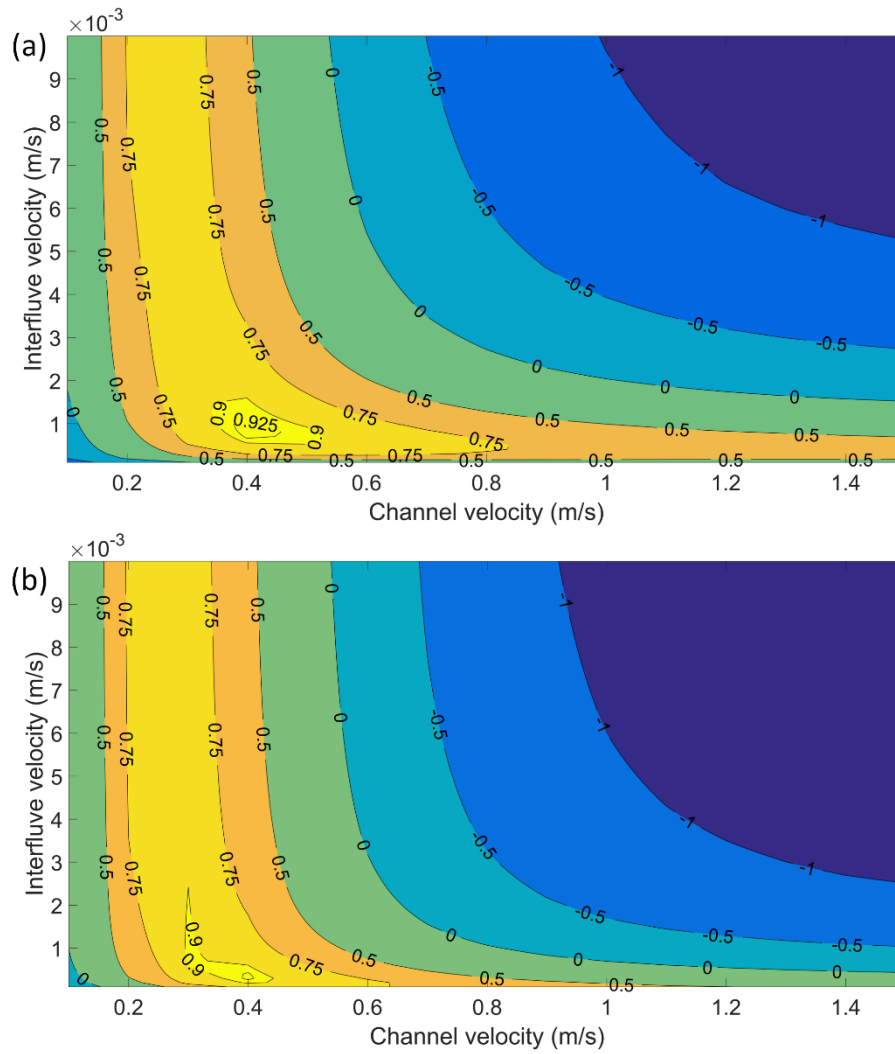


Figure 5. Calibration of channel and interfluvial velocities using (a) conservative and (b) non-conservative supraglacial river delineations. Contour labels show Nash-Sutcliffe model efficiencies (*NSEs*) obtained by applying different combinations of mean interfluvial (v_h) and open-channel velocities (v_c) and comparing with the field-measured hydrograph just upstream of the Rio Behar catchment terminal outlet moulin.

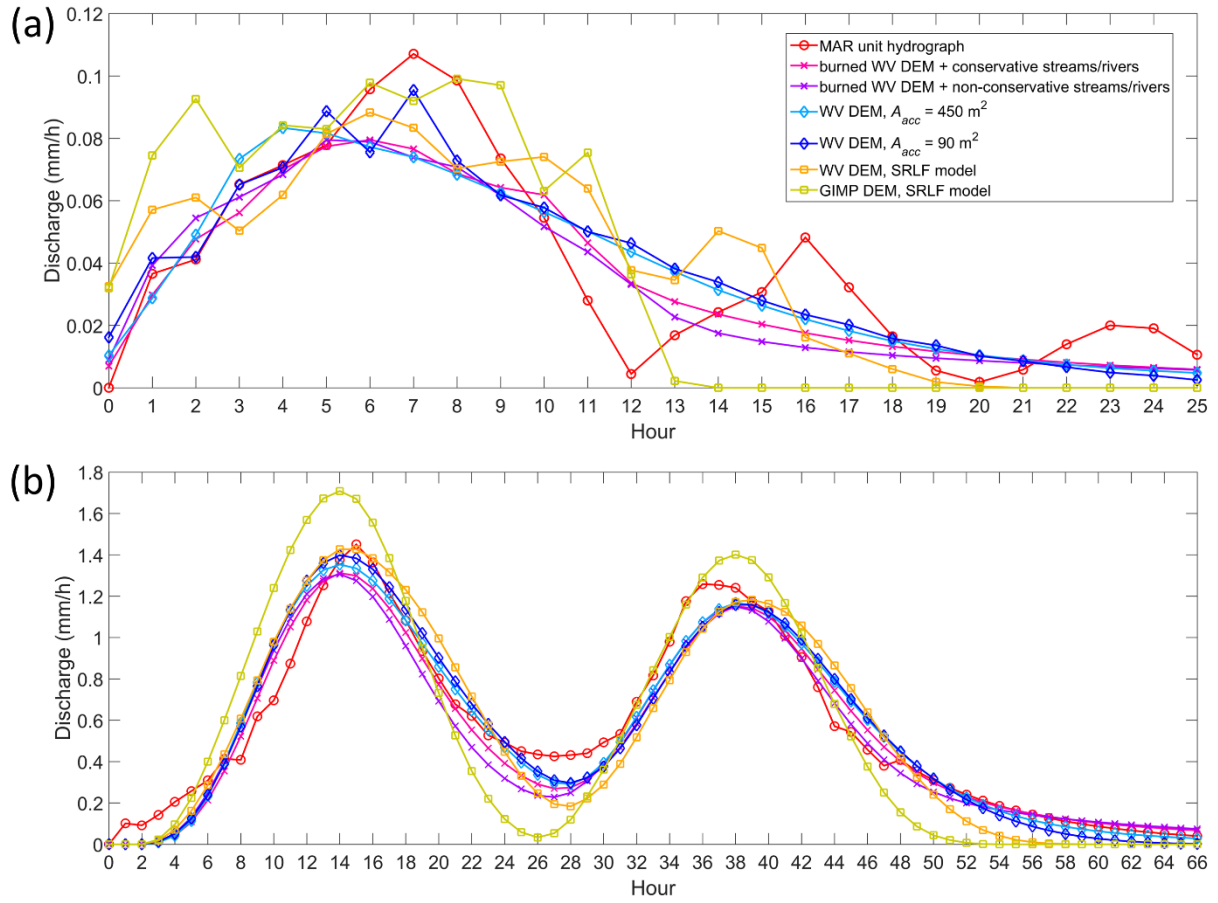


Figure 6. (a) Unit hydrographs (UHs) and (b) simulated direct hydrographs at the terminal moulin of the Rio Behar catchment, as modeled by different data sources and methods. The MAR UH is calibrated from effective MAR melt and measured supraglacial river discharge (Fig. 2). The Rescaled Width Function (RWF) and surface routing and lake filling (SRLF) UHs are obtained by

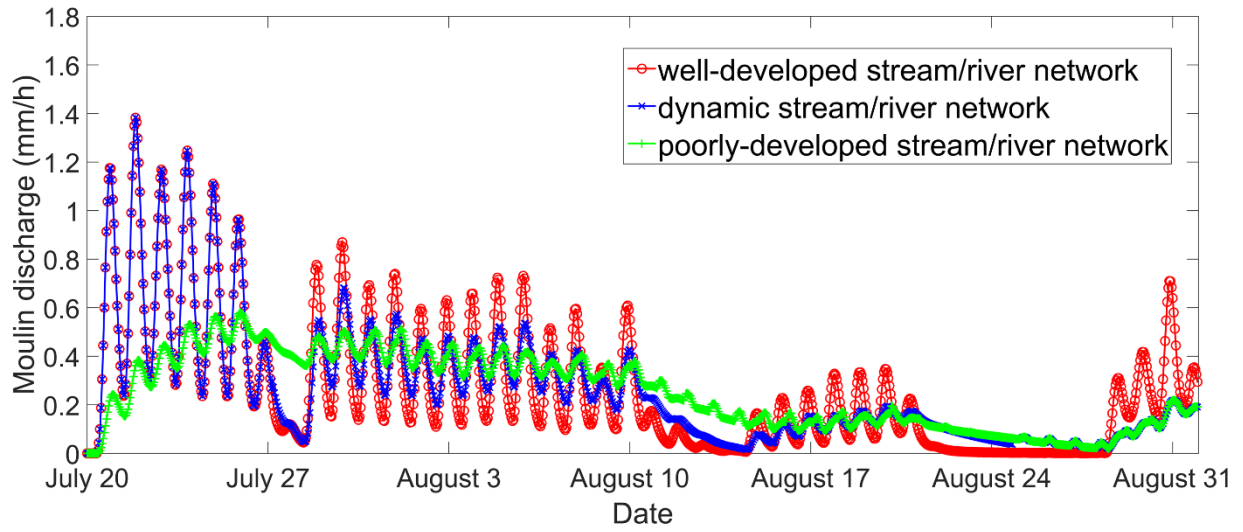


Figure 7. Simulated Rio Behar catchment discharge at the terminal outlet moulin for 20 July to 31 August 2015 assuming a seasonally evolving supraglacial stream/river network. A series of contributing area thresholds (A_c) of 250, 500, 1000, 2500, and 5000 pixels is used to mimic an evolving supraglacial stream/river drainage network from the 18 July 2015 WorldView DEM. The minimum A_c (250 pixels) is used to simulate well-developed river networks, while the maximum A_c (5000 pixels) is used to simulate poorly-developed river networks. Variable A_c values are used to simulate dynamic river networks, which are considered best capturing realistic seasonal evolution. Drainage density is lowest in early and late season, and highest in July. The diurnal variations of moulin discharge are strongly controlled by supraglacial stream/river network patterns.

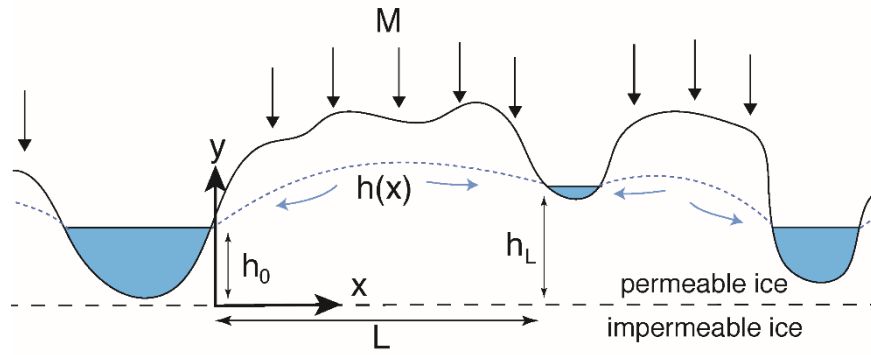


Figure 8. Schematic diagram of subsurface meltwater porous flow through weathering crust and permeable near-surface, low density ice to estimate interfluvial transport speed v_h . Melt generated at the near surface at rate M percolates through porous ice, supplying a water table that transports melt downhill towards streams at heights h_0 and h_L above a layer of impermeable ice (dashed line).

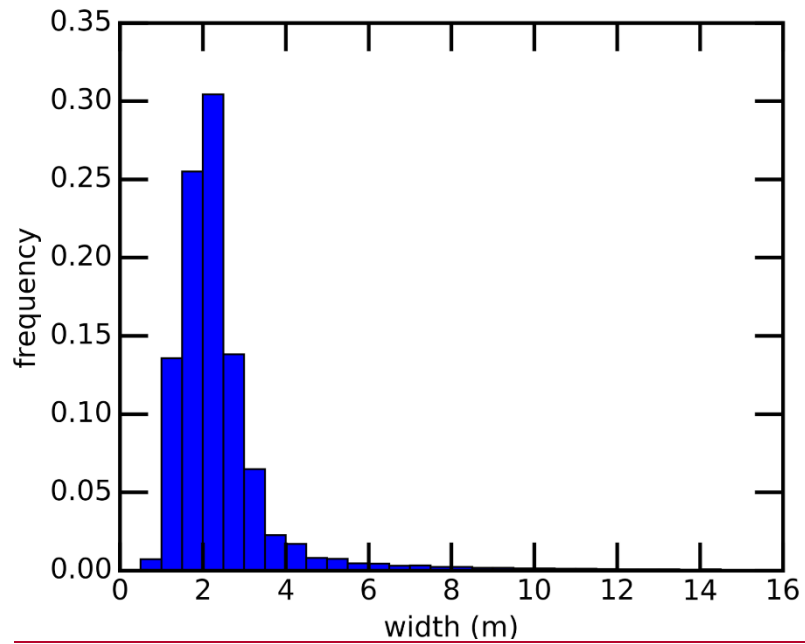


Figure 9. Channel width histogram of conservatively mapped supraglacial stream/river networks in Rio Behar catchment. Most supraglacial meltwater channels are narrower than 4 m with a mean width of 2.5 ± 2.0 m, confirming that numerous small supraglacial streams dominate the bulk-catchment average channel velocity v_c .

Table I. Surface meltwater travel distances, velocities, and times in the Rio Behar catchment for July 2015.

| Input data sources | Mean L_c (k 10^3 m) | Mean L_h (m) | Optimal v_c (m/s) | Optimal v_h (10^{-3} m/s) | Mean v | NSE | Mean t_c (hour) | Mean t_h (hour) |
|---|--|-------------------|------------------------|-----------------------------------|---------------|----------------|----------------------|----------------------|
| Burned WV DEM, conservative threshold | 7.1 ± 4.0 | 19.7 ± 30.9 | 0.4 | 0.9 | - | 0.9443 | 4.9 ± 2.8 | 6.1 ± 9.5 |
| | | | 0.4 | 0.7-1.2 | - | >0.9250 | | |
| | | | 0.3-0.5 | 0.5-1.5 | - | >0.9000 | | |
| Burned WV DEM, non-conservative threshold | 7.5 ± 4.4 | 6.7 ± 15.0 | 0.4 | 0.3 | - | 0.9324 | 5.2 ± 3.1 | 6.2 ± 13.9 |
| | | | 0.4 | 0.3-0.4 | - | >0.9250 | | |
| | | | 0.3-0.5 | 0.2-2.0 | - | >0.9000 | | |
| WV DEM, $A_c = 50$ pixels | 6.8 ± 3.8 | 22.8 ± 22.2 | 0.8 | 0.9 | - | 0.9396 | 2.4 ± 1.3 | 7.0 ± 6.9 |
| | | | 0.6-1.5 | 0.8-1.0 | - | >0.9250 | | |
| | | | 0.5-2.0 | 0.7-1.2 | - | >0.9000 | | |
| WV DEM, $A_c = 10$ pixels | 6.8 ± 3.8 | 8.7 ± 9.0 | 0.5 | 0.5 | - | 0.9362 | 3.8 ± 2.1 | 4.8 ± 5.0 |
| | | | 0.5-0.6 | 0.4-0.5 | - | >0.9250 | | |
| | | | 0.4-0.8 | 0.3-0.6 | - | >0.9000 | | |
| WV DEM, SRLF method | - | - | - | - | 0.3 ± 0.1 | 0.8742 | - | - |
| 30 m GIMP v2, SRLF method | - | - | - | - | 0.3 ± 0.1 | 0.7068 | - | - |